

Gravitational Lensing and Dark Matter

Yannick Mellier

IAP Paris and CEA/IRFU Saclay

Multiple images: the « Einstein Cross »

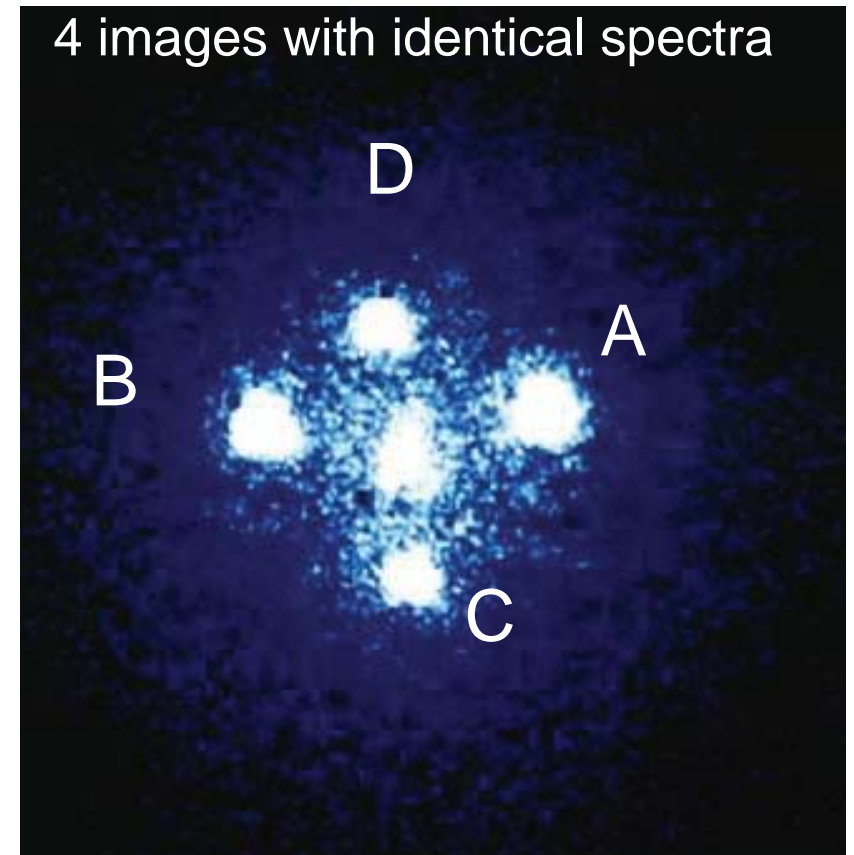
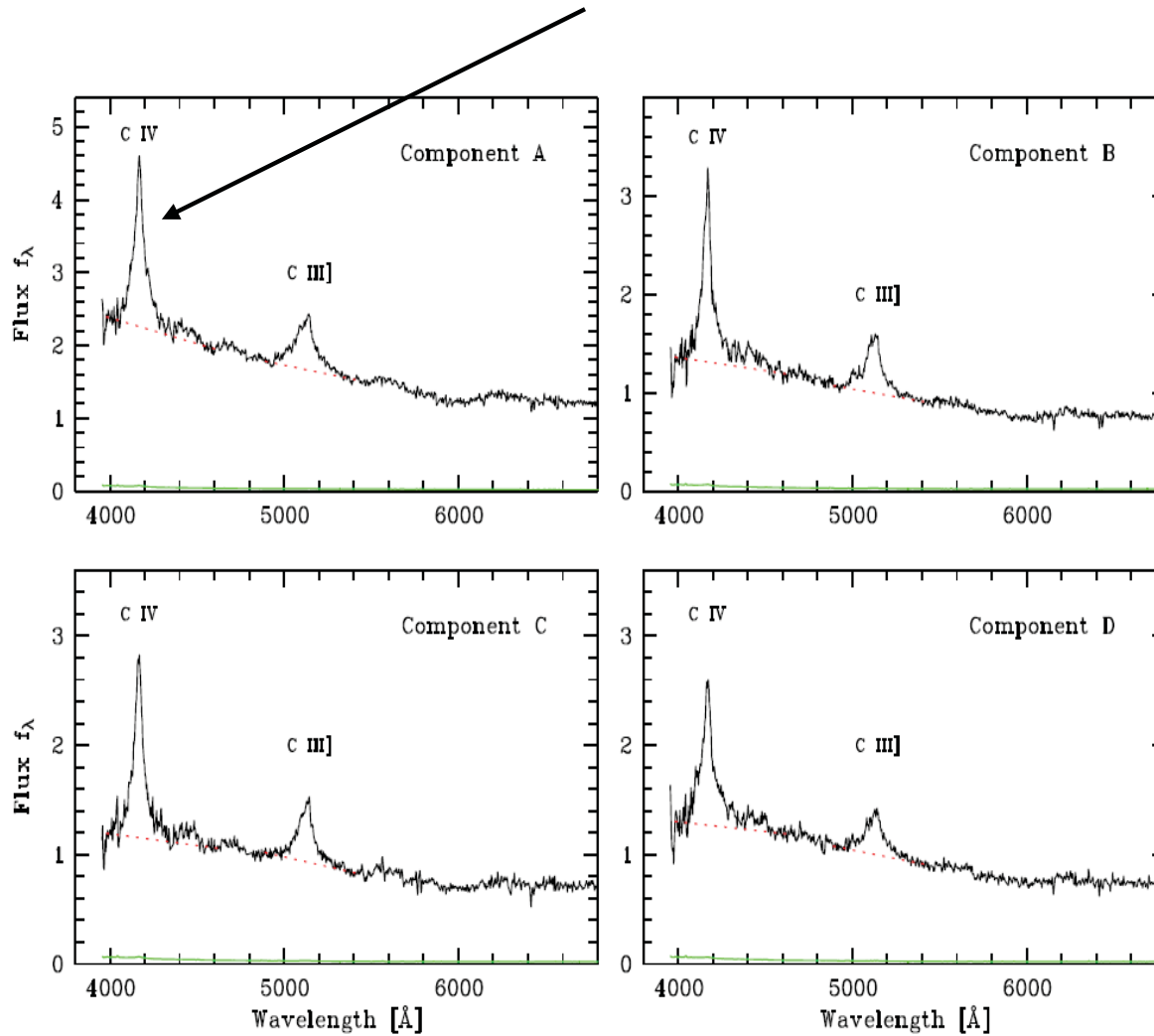
Galaxy 2227+030

Redshift $z=0.0394$



The « Einstein Cross »

CIV emission line at 154.9 nm observed 417.6 nm : $z = 1.695$



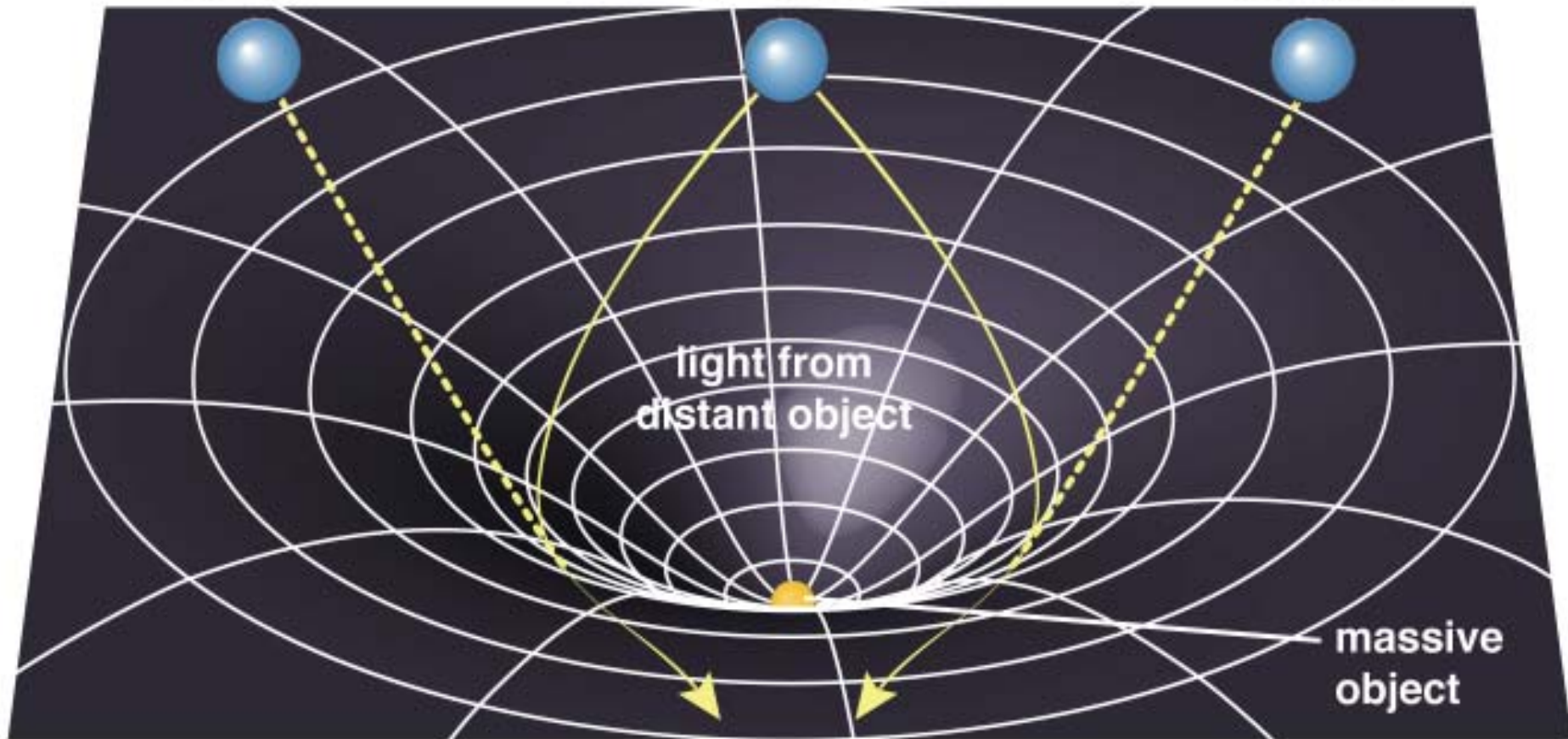
General relativity:

curvature of space time locally modified by mass condensation

Apparent position of a first image
image 1

Real image
real object

Apparent position of a second image
image 2



Deflection of light, magnification, image multiplication distortion of objects : directly **depend on the amount of matter**

Gravitational lensing effect is **achromatic** (photons follow geodesics regardless their energy)

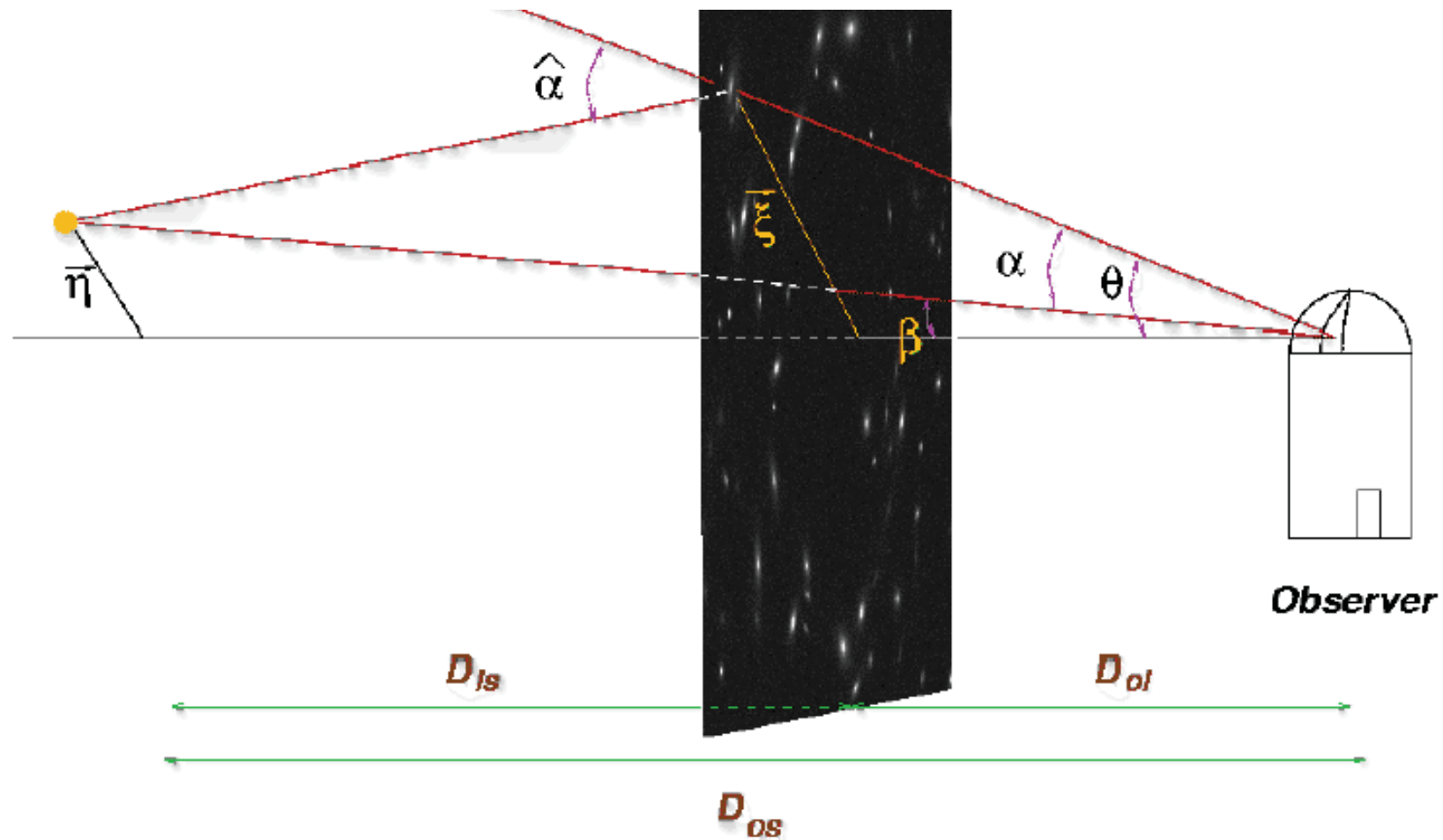
Gravitational Lensing

theory, concepts and definitions

Gravitational lensing: fundamental assumptions

- Weak field limit: $\sigma^2 \ll c^2$
- Stationnary field: $t_{\text{dyn}} \sim R_{\text{lens}}/v \gg t_{\text{cross-photon}}$
- Thin lens approximation: $R_{\text{lens}} \ll R_{\text{bench}}$
- Small deflection angle:
 $b = \text{impact parameter ; } R = \text{Schwarzschild radius}$
 $\alpha = 4G M/bc^2 \ll 2G M/R_S c^2$
 $\Rightarrow R_S \ll b$
- Transparent lens

Lens equation and deflection angle



$$\vec{\eta} = \frac{D_{os}}{D_{ol}} \vec{\xi} - D_{ls} \hat{\alpha} \left(\vec{\xi} \right) \quad ; \quad \alpha = -\frac{2}{c^2} \int_S^O \nabla_{\perp} \Phi \, dl$$

Deflection angle and mass density

$$\alpha = -\frac{2}{c^2} \int_S \nabla_{\perp} \Phi \, dl$$

$$\alpha(\xi) = \frac{4G}{c^2} \int \frac{(\xi - \xi') \Sigma(\xi')}{|\xi - \xi'|^2} d\xi'$$

where

- $\Sigma(\xi)$ is the projected mass density,
- ξ is a 2-dimensional vector in the lens plane and
- the integration is done over the lens plane.

Lens equation : spherical lens

- Lens equation

$$\vec{\eta} = \frac{D_{os}}{D_{ol}} \vec{\xi} - D_{ls} \hat{\vec{\alpha}} \left(\vec{\xi} \right)$$

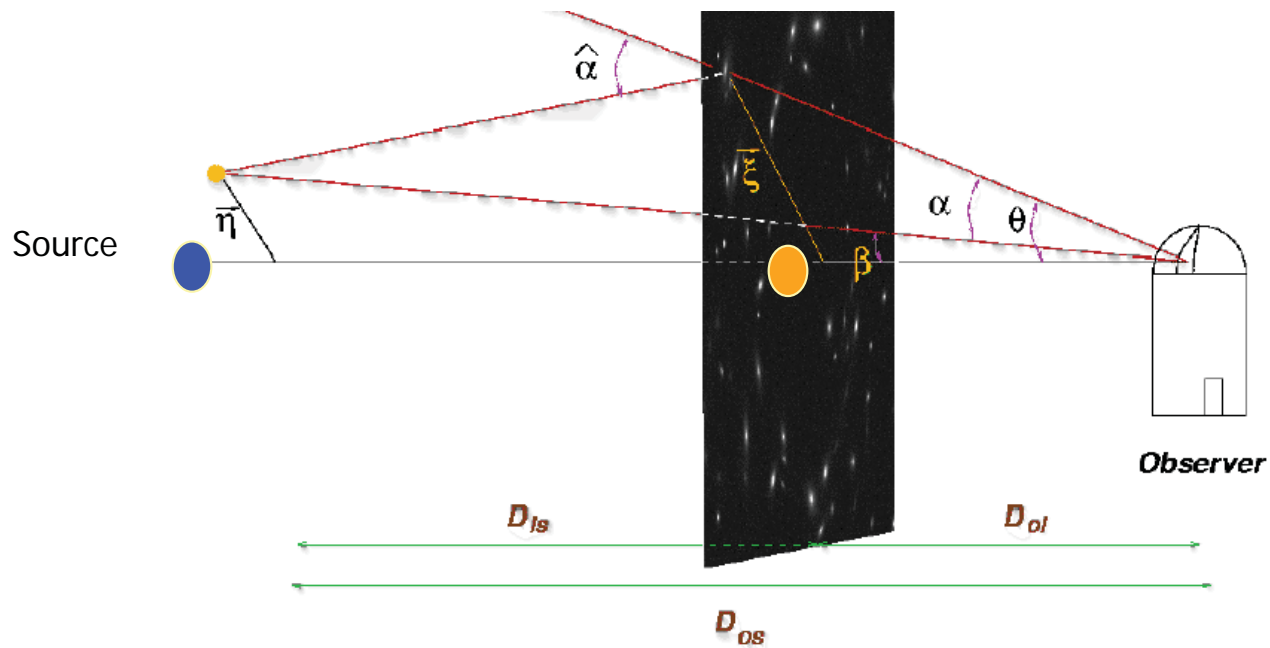
Setting $\vec{\eta} = D_{os} \vec{\beta}$ and $\vec{\xi} = D_{ol} \vec{\theta}$,

$$\vec{\beta} = \vec{\theta} - \vec{\alpha} \left(\vec{\theta} \right)$$

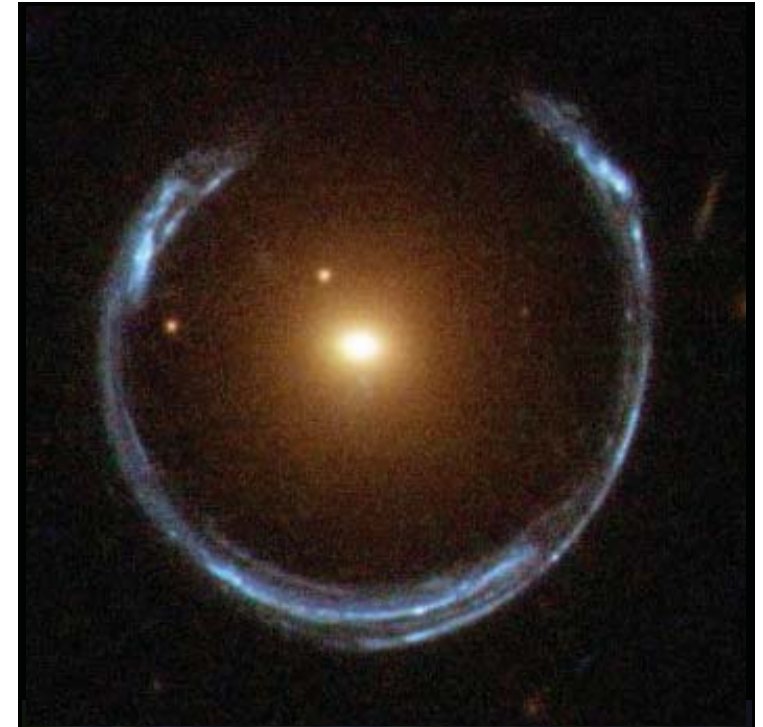
- Spherically symmetric lens

$$\beta = \theta - \frac{D_{ls}}{D_{os} D_{ol}} \frac{4GM(\theta)}{c^2 \theta}$$

Perfect lens configuration « Einstein ring »



Source-Lens-Observer perfectly aligned



Einstein ring

$$\theta_E = \left(\frac{D_{ls}}{D_{os}D_{ol}} \frac{4GM(\theta_E)}{c^2} \right)^{1/2}$$

Typical values:

- For a lens of 1 solar mass located at 1 AU and a source a 1 kpc
 $\theta_E = 0.003$ arc-second
- For a lens of 10^{11} solar masses located at 100kpc and a source at 300 kpc
 $\theta_E = 1$ arc-second
- For a lens of 10^{15} solar masses located at 1Gpc and a source at 3 Gpc
 $\theta_E = 30$ arc-second (sensitive to cosmological parameters)

Convergence and critical density

- **Convergence and critical density** The gravitational convergence is a dimensionless surface mass density:

$$\kappa(\vec{\theta}) = \frac{\Sigma(D_{ol}\vec{\theta})}{\Sigma_{cr}}$$

where Σ_{crit} is the *critical surface mass density*:

$$\Sigma_{cr} = \frac{c^2}{4\pi G} \frac{D_{os}}{D_{ol}D_{ls}}$$

that defined a "strength" of the lens. Strong lensing cases have $\Sigma > \Sigma_{cr}$

Magnification and distortion

$$\vec{\beta} = \vec{\theta} - \vec{\alpha}(\vec{\theta}) \quad \alpha = -\frac{2}{c^2} \int_S^O \nabla_{\perp} \Phi \, dl$$

- Jacobian of the lens mapping. Differentiating the lens equation

$$A(\vec{\theta}) = \frac{\partial \vec{\beta}}{\partial \theta} = \left(\delta_{ij} - \frac{\partial^2 \psi(\vec{\theta})}{\partial \theta_i \partial \theta_j} \right) = M^{-1}$$

- Convergence, Shear

$$\begin{cases} \kappa = \frac{1}{2}(\psi_{,11} + \psi_{,22}) \\ \gamma_1(\vec{\theta}) = \frac{1}{2}(\psi_{,11} - \psi_{,22}) = \gamma(\vec{\theta}) \cos[2\varphi(\vec{\theta})] \\ \gamma_2(\vec{\theta}) = \psi_{,12} = \gamma(\vec{\theta}) \sin[2\varphi(\vec{\theta})] \end{cases}$$

Magnification and distortion

- Magnification, Convergence, Shear

$$A = \mathcal{M}^{-1} = \begin{pmatrix} 1 - \kappa - \gamma_1 & -\gamma_2 \\ -\gamma_2 & 1 - \kappa + \gamma_1 \end{pmatrix}$$

$$\mathcal{M}^{-1} = (1 - \kappa) \begin{pmatrix} 1 & 0 \\ 0 & 1 \end{pmatrix} - \gamma \begin{pmatrix} \cos(2\varphi) & \sin(2\varphi) \\ \sin(2\varphi) & -\cos(2\varphi) \end{pmatrix}$$

where $\gamma = \gamma_1 + i\gamma_2 = |\gamma|e^{2i\varphi}$

- Amplification amplitude

$$\mu = (\det A)^{-1} = \frac{1}{\left[(1 - \kappa)^2 - |\gamma|^2 \right]}$$

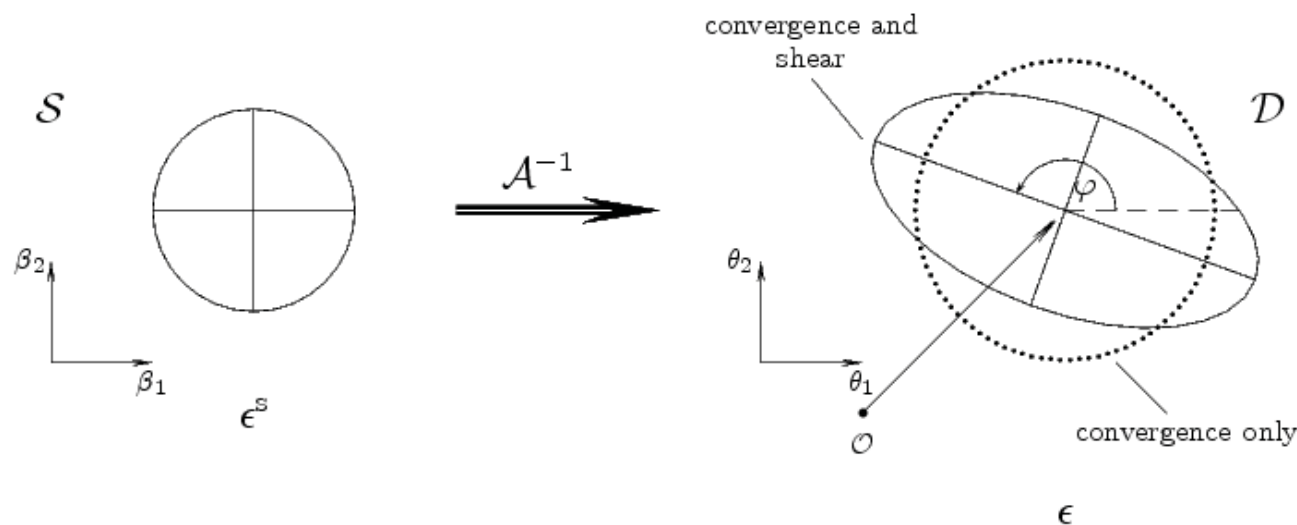
- Eigenvalues of \mathcal{M}^{-1} :

$$1 - \kappa + \gamma, \quad 1 - \kappa - \gamma$$

Magnification and distortion

- **Image and source** From the magnification matrix,
 - κ expresses an isotropic magnification. It transforms a circle into a larger/smaller circle.
 - γ is an anisotropic magnification. It transforms a circle into an ellipse with minor and major axes :

$$b = (1 - \kappa + \gamma)^{-1} , \quad a = (1 - \kappa - \gamma)^{-1}$$



From (reduced) shear to ellipticity

- **Reduced shear** Let us write the magnification matrix as:

$$A = \mathcal{M}^{-1} = (1 - \kappa) \begin{pmatrix} 1 - g_1 & -g_2 \\ -g_2 & 1 + g_1 \end{pmatrix}$$

where

$$g(\vec{\theta}) = \frac{\gamma(\vec{\theta})}{1 - \kappa(\vec{\theta})} = g_1 + ig_2 = |g|e^{2i\varphi}$$

is the *reduced shear*. It directly provides the image ellipticity induced by lensing on a circular source:

$$\frac{b}{a} = \frac{1 - |g|}{1 + |g|}$$

as well as the orientation of the major axis, φ .

→ Measuring ellipticity=measuring gravitational shear

Caustic and critical lines

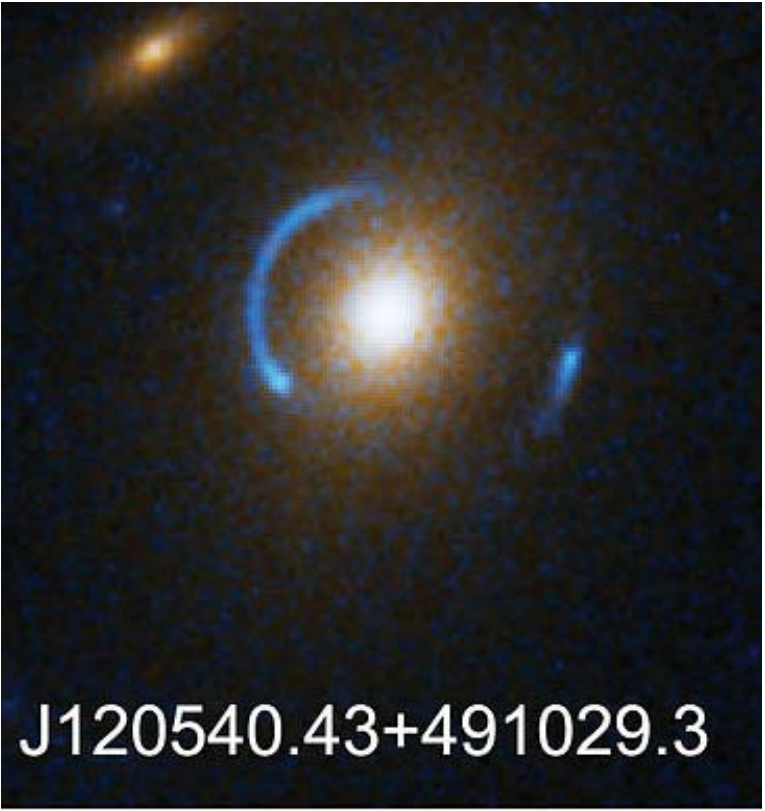
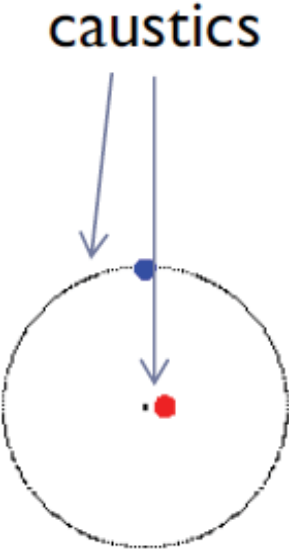
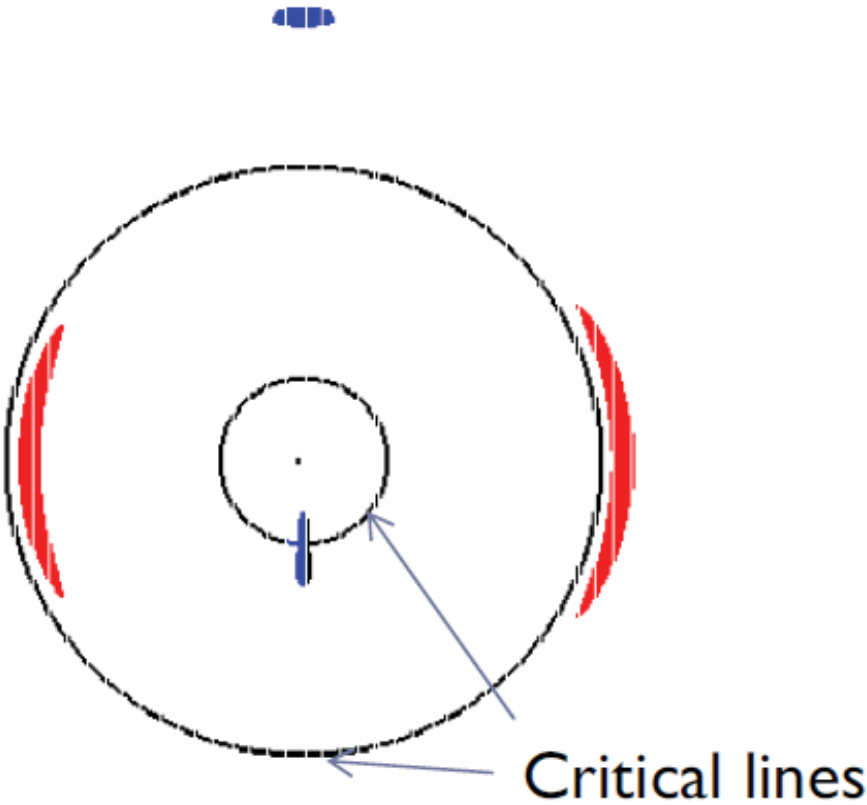
- Amplification amplitude

$$\mu = (\det A)^{-1} = \frac{1}{\left[(1 - \kappa)^2 - |\gamma|^2 \right]}$$

- critical lines corresponds to positions in the lens plane with $\det A = 0$
- the corresponding positions on the source plane are the caustic lines
- the positions of source points with respect to a caustic lines define the number of image multiplication and the source magnification
- when a source crosses a caustic line, its amplification is almost infinity, and image pairs are formed

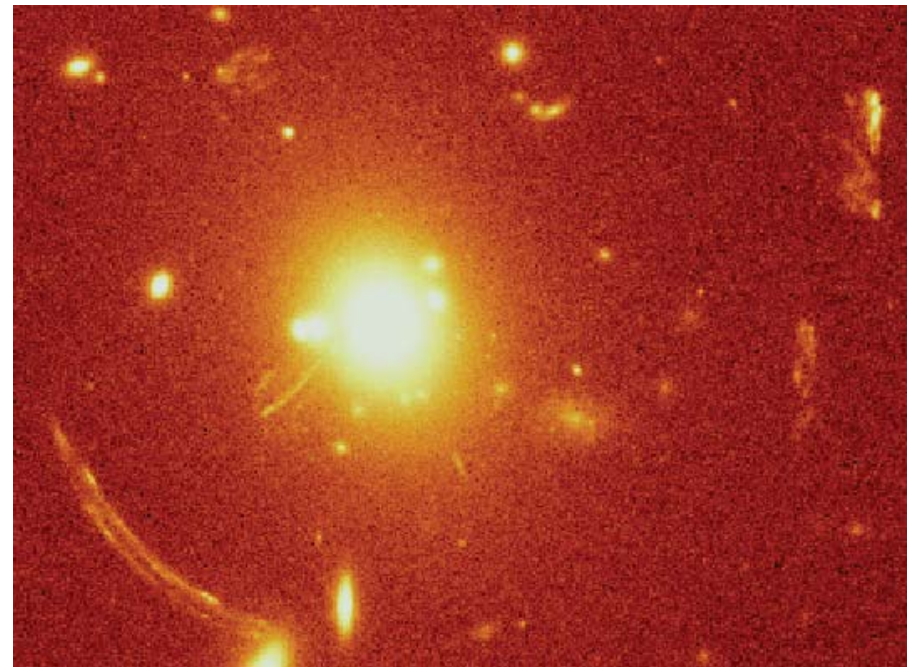
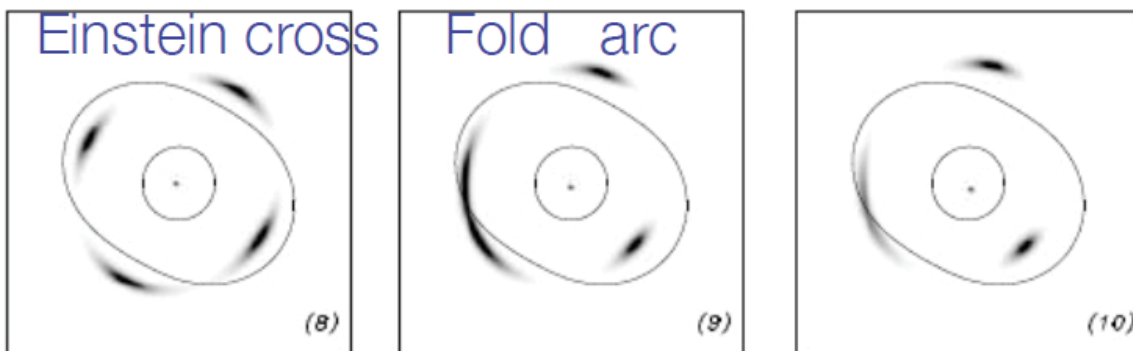
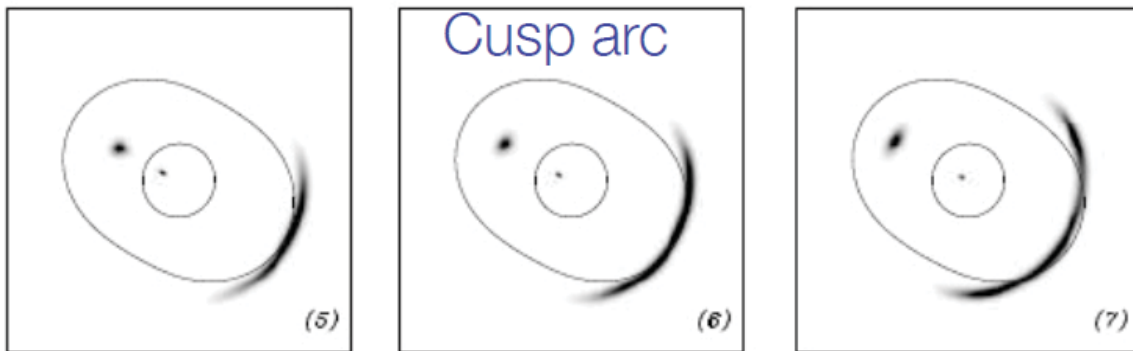
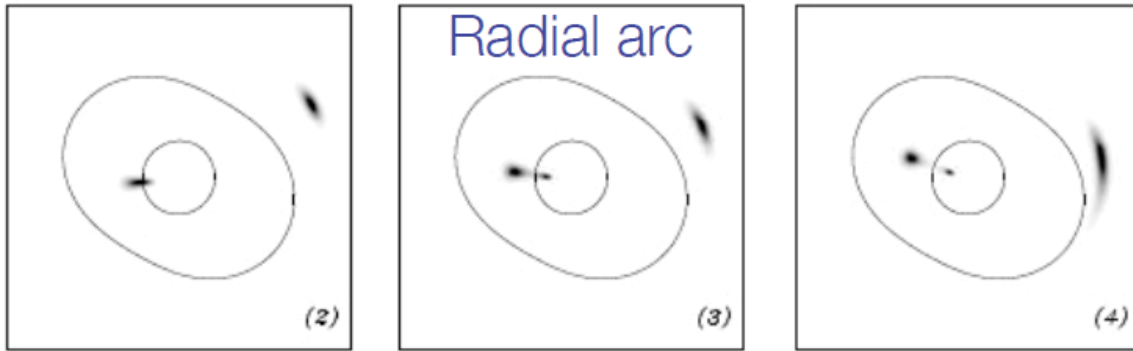
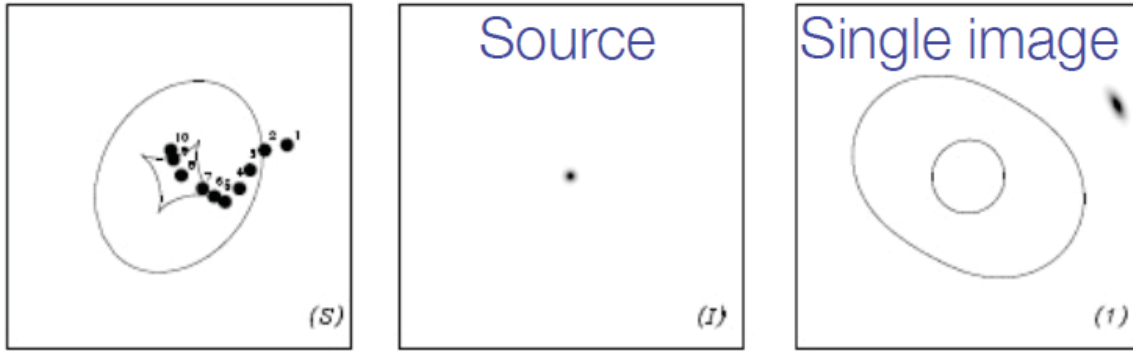
Caustic lines and critical lines

Circular potential with core



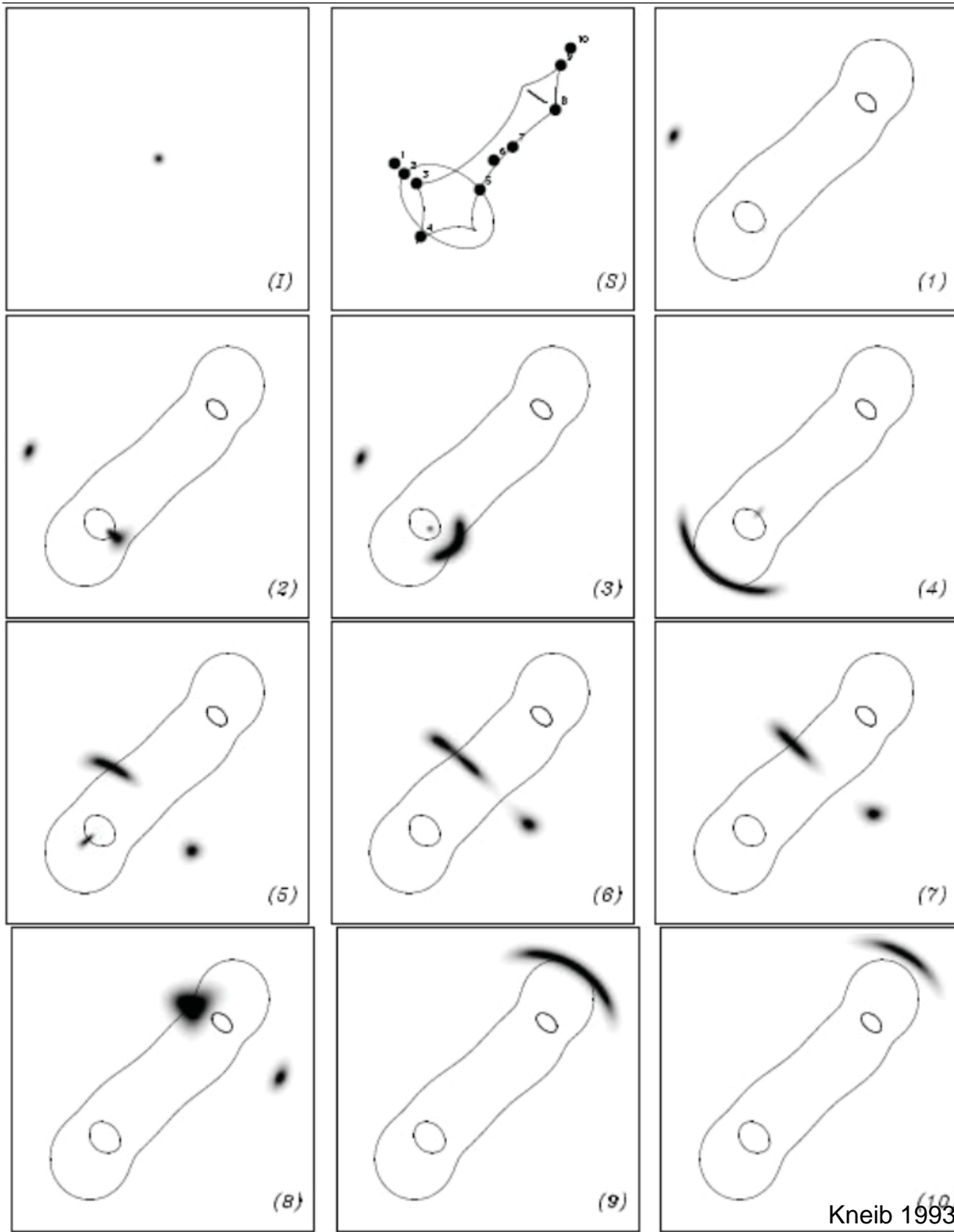
Caustic and critical lines

Elliptical potential with core



Caustic and critical lines

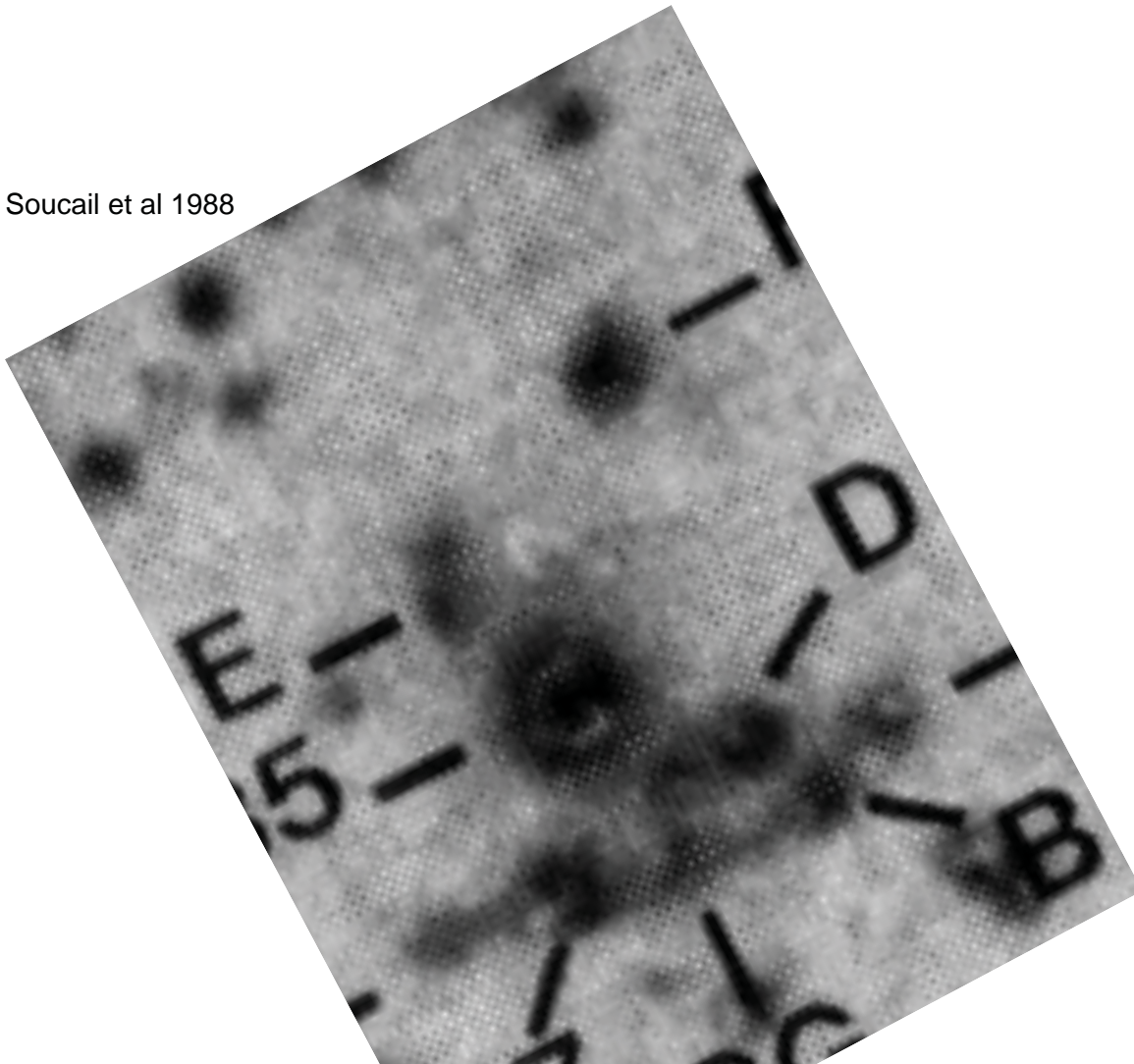
Bimodal potential
with core



Dark matter with Strong Gravitational Lensing

Abell 370: first gravitational arc discovered

Soucail et al 1988

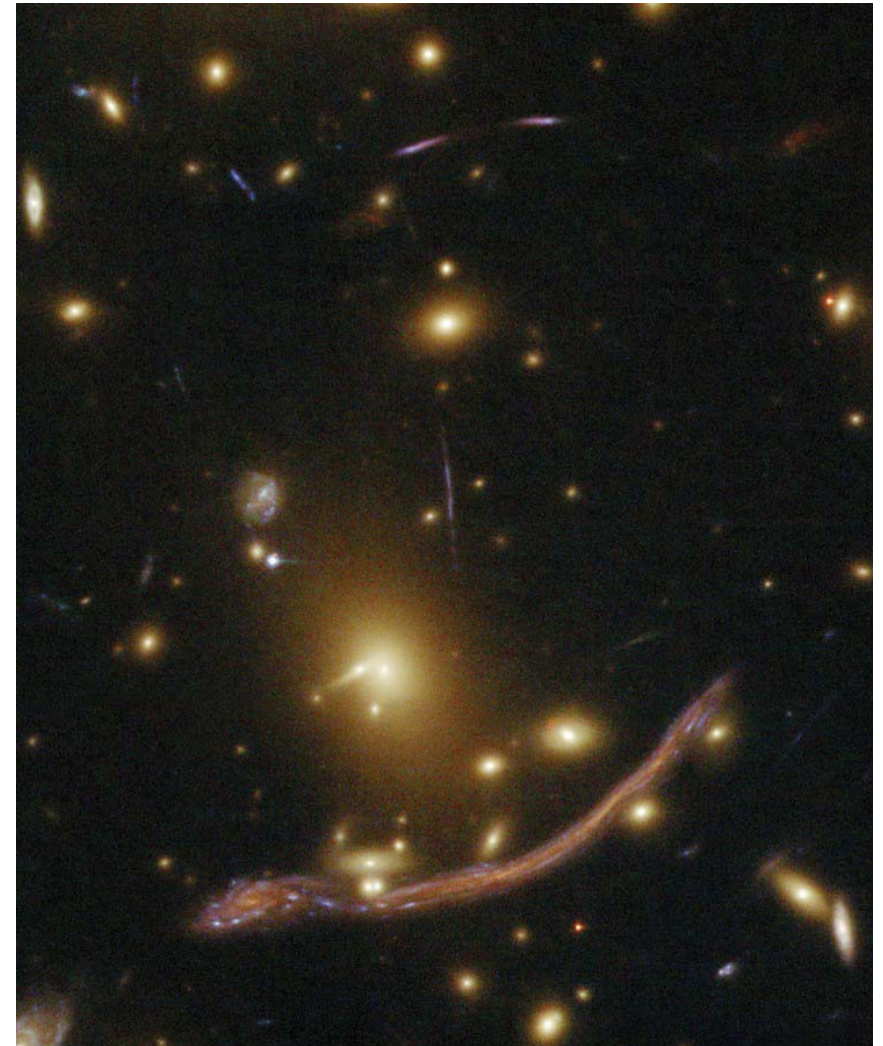


6 Sept. 1985 - A370 arc discovery

Very 1st image at CFHT Cass. focus

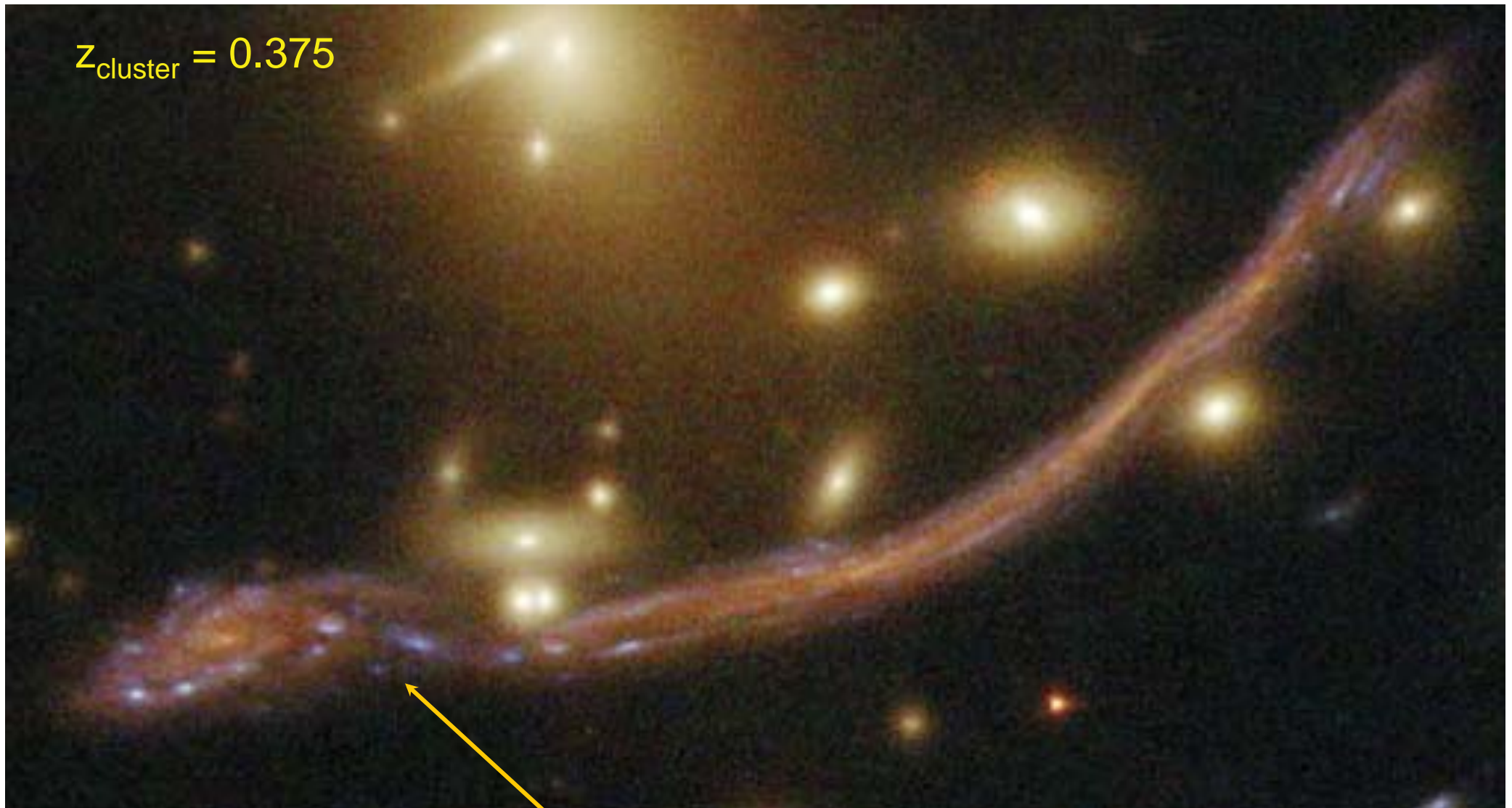
RCA 512x320 CCD 0.8" /pixel,

10mn R-band , seeing 0.8"



Abell 370, HST/ACS ; credit NASA/ESA

Abell 370: first gravitational arc discovered



$z_{\text{cluster}} = 0.375$

A spiral structure resolved at $z=0.724$

Abell 370, HST/ACS ; credit NASA/ESA

Abell 370: singular isothermal sphere model

Lens equation:

$$\theta_S = \theta_I - 4\pi \frac{\sigma^2}{c^2} \frac{D_{LS}}{D_{OS}} \frac{\theta_I}{|\theta_I|}$$

Effective potential:

$$\varphi = 4\pi \frac{\sigma^2}{c^2} \frac{D_{LS}}{D_{OS}} r$$

Magnification matrix:

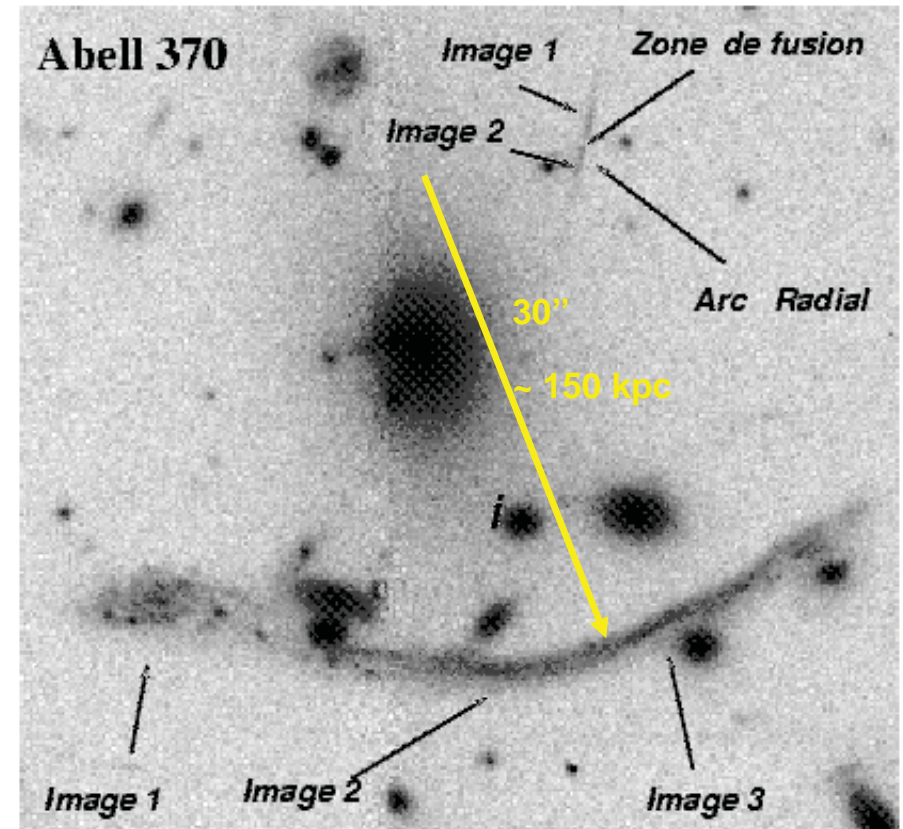
$$\begin{pmatrix} 1 & 0 \\ 0 & 1 - 4\pi \frac{\sigma^2}{c^2} \frac{D_{LS}}{D_{OS}} \frac{1}{|\theta_I|} \end{pmatrix}$$

Deflection angle:

$$\theta_{SIS} = 4\pi \frac{\sigma^2}{c^2} \frac{D_{LS}}{D_{OS}} \approx 16'' \left(\frac{\sigma}{1000 \text{ km} \cdot \text{sec}^{-1}} \right)^2$$

Total mass inside the Einstein radius:

$$M(\theta) = 0.57 \times 10^{14} h^{-1} M_{\odot} \left(\frac{\theta}{30''} \right) \left(\frac{\sigma}{1000 \text{ km} \cdot \text{sec}^{-1}} \right)^2$$



Kneib et al 94

MS2137-23

A

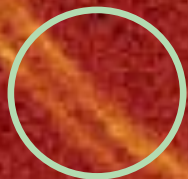
B

A

B

A

A

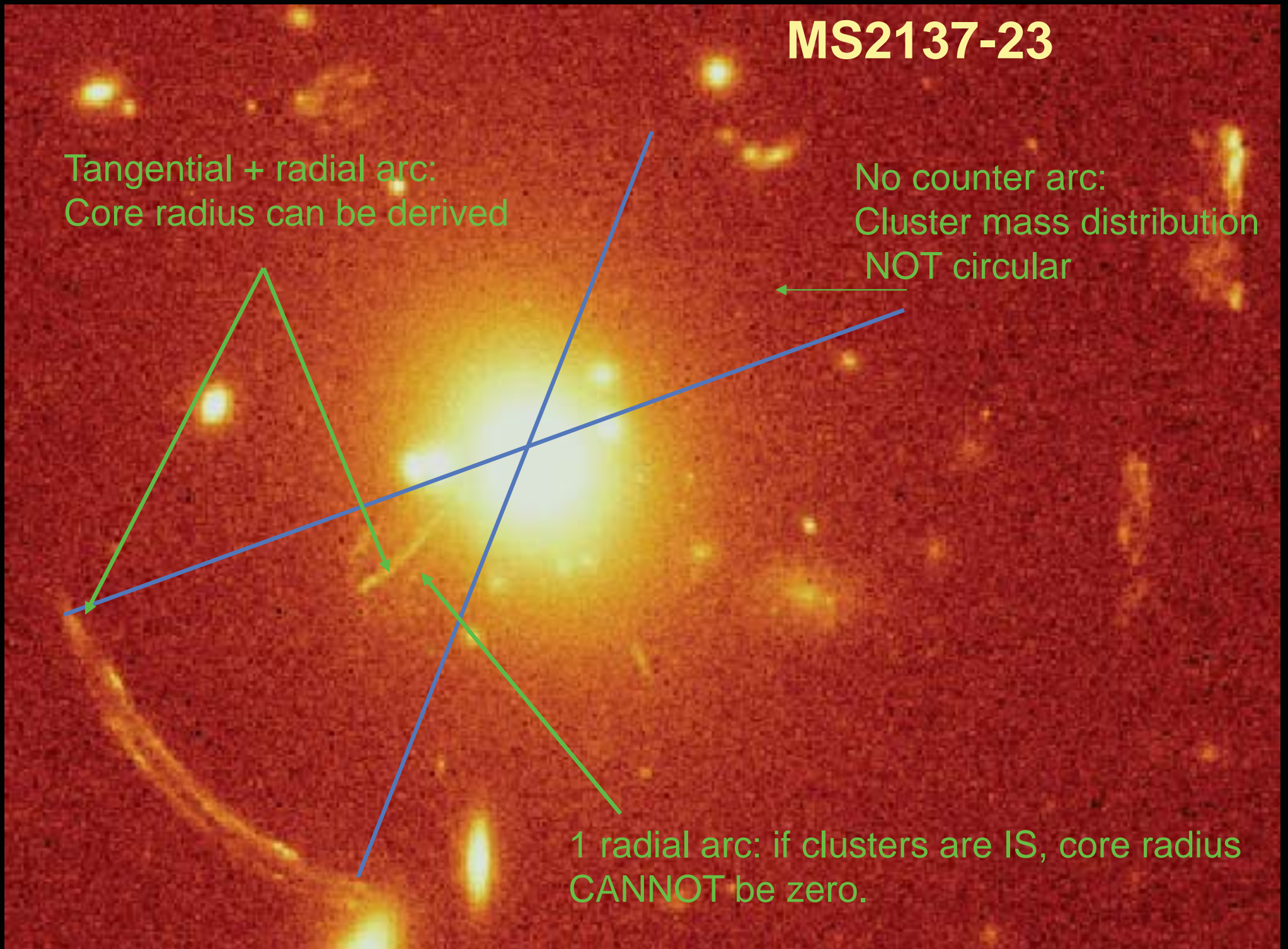


MS2137-23

Tangential + radial arc:
Core radius can be derived

No counter arc:
Cluster mass distribution
NOT circular

1 radial arc: if clusters are IS, core radius
CANNOT be zero.



Modelling strong lenses

Constraints :

- The angular lens equation set the relation between each image position, $\theta_i^I, \theta_j^I, \theta_k^I, \dots$, and the unique position back in the source plane:

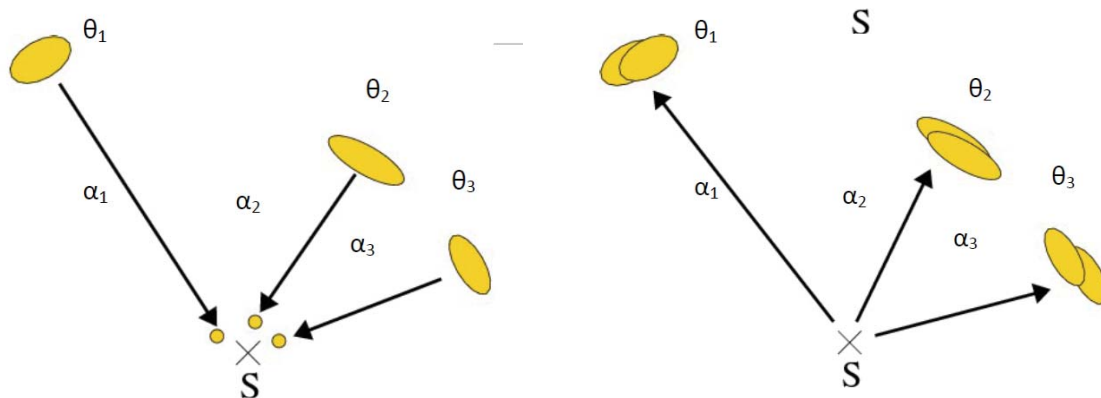
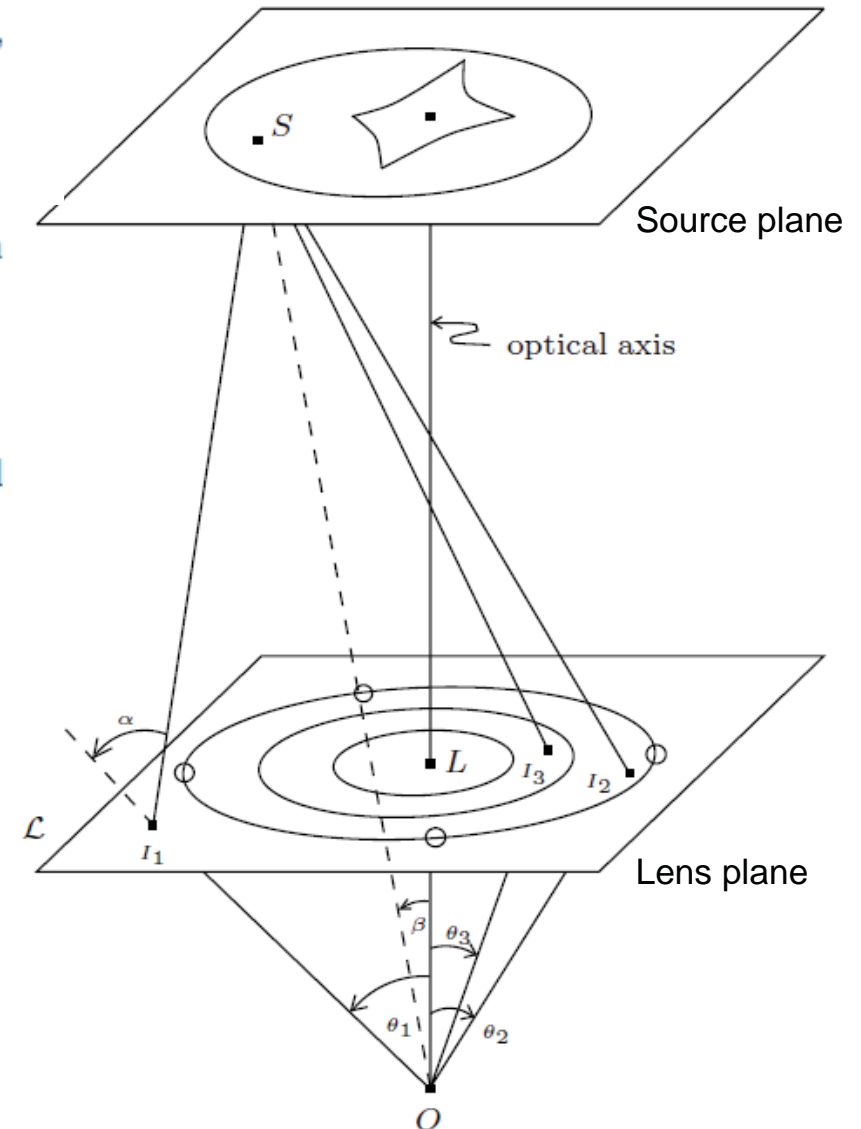
$$\theta^S = \theta_i^I - \alpha(\theta_i^I) = \theta_j^I - \alpha(\theta_j^I) = \theta_k^I - \alpha(\theta_k^I) = \dots$$

- The flux ratios between each image is an estimate of their magnification ratio:

$$\frac{F_i^I}{F_j^I} = \frac{|\mu_i^I|}{|\mu_j^I|} ; \frac{F_i^I}{F_k^I} = \frac{|\mu_i^I|}{|\mu_k^I|} ; \dots$$

- When sent back to the source plane, the morphology of each un-lensed image should be identical.

Method : mapping, inversion



MS2137-23 mass model

from critical lines analysis

$$\Phi(r, \theta) = \Phi_0 \sqrt{1 + \left(\frac{r}{r_c}\right)^2 (1 - \epsilon \cos 2\theta)}.$$

$$\mathbf{M}^{-1} = \begin{pmatrix} 1 - \frac{1}{r} \frac{\partial \Phi}{\partial r} - \frac{1}{r^2} \frac{\partial^2 \Phi}{\partial \theta^2} & -\frac{\partial}{\partial r} \left(\frac{1}{r} \frac{\partial \Phi}{\partial \theta} \right) \\ -\frac{\partial}{\partial r} \left(\frac{1}{r} \frac{\partial \Phi}{\partial \theta} \right) & 1 - \frac{\partial^2 \Phi}{\partial r^2} \end{pmatrix}.$$

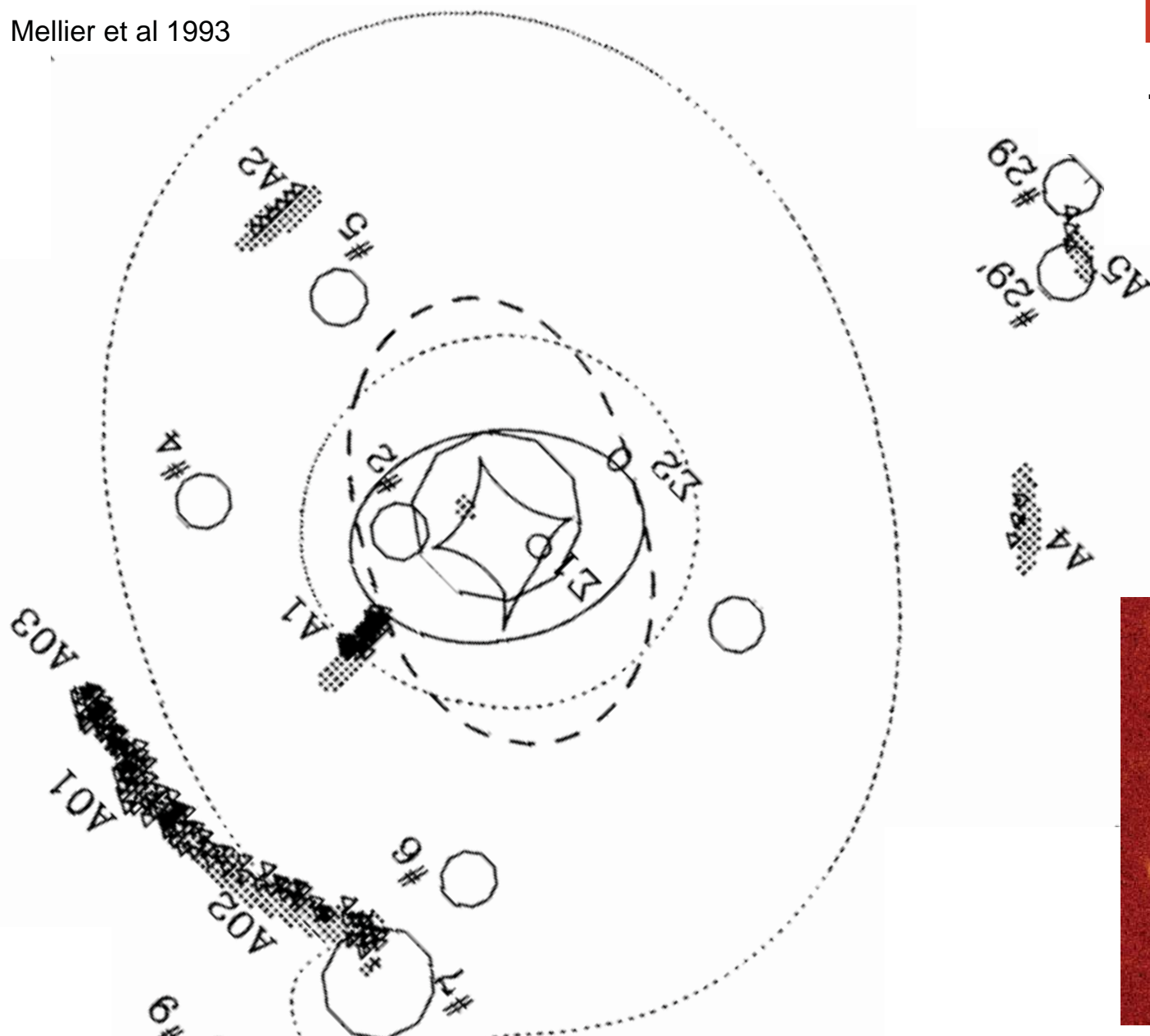
Small ellipticity and small core radius: $\frac{\partial}{\partial r} \left(\frac{1}{r} \frac{\partial \Phi}{\partial \theta} \right) \sim 0$

Tangential critical line: $1 - \frac{1}{r} \frac{\partial \Phi}{\partial r} - \frac{1}{r^2} \frac{\partial^2 \Phi}{\partial \theta^2} = 0.$

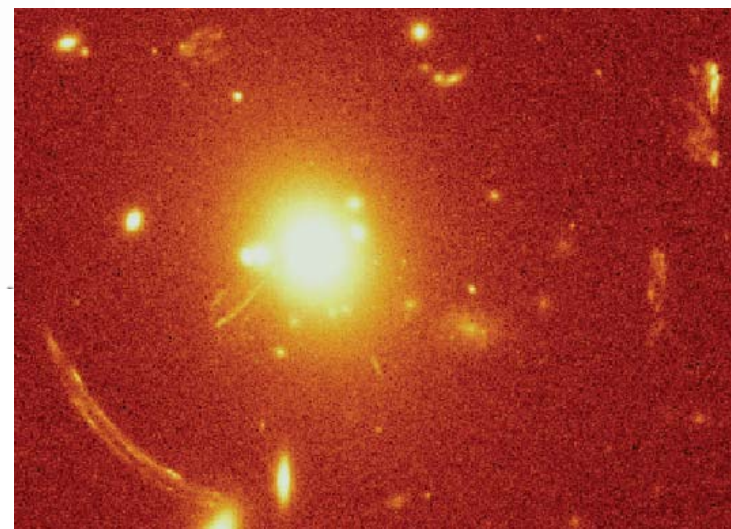
Radial critical line: $1 - \frac{\partial^2 \Phi}{\partial r^2} = 0.$

| System | ϵ | θ | r_c | σ_{los} (km s $^{-1}$) |
|-----------------------------|------------------------|--------------------------|-------------------|---------------------------------------|
| Cluster model | $0.08^{+0.03}_{-0.03}$ | $29^{\circ}.5^{+9}_{-5}$ | $8''^{+0.5}_{-2}$ | 1000 |
| cD ^a | 0.07 ± 0.04 | $29^{\circ}.5 \pm 5$ | 1.5 ± 1 | 350 ± 30^b |
| Galaxy 7 model | 0.04 | 8 | 0 $^{\circ}$.27 | 185 |
| Galaxy 7 ^a | 0.07 | 8 | ... | 230 ± 30^b |

Mellier et al 1993

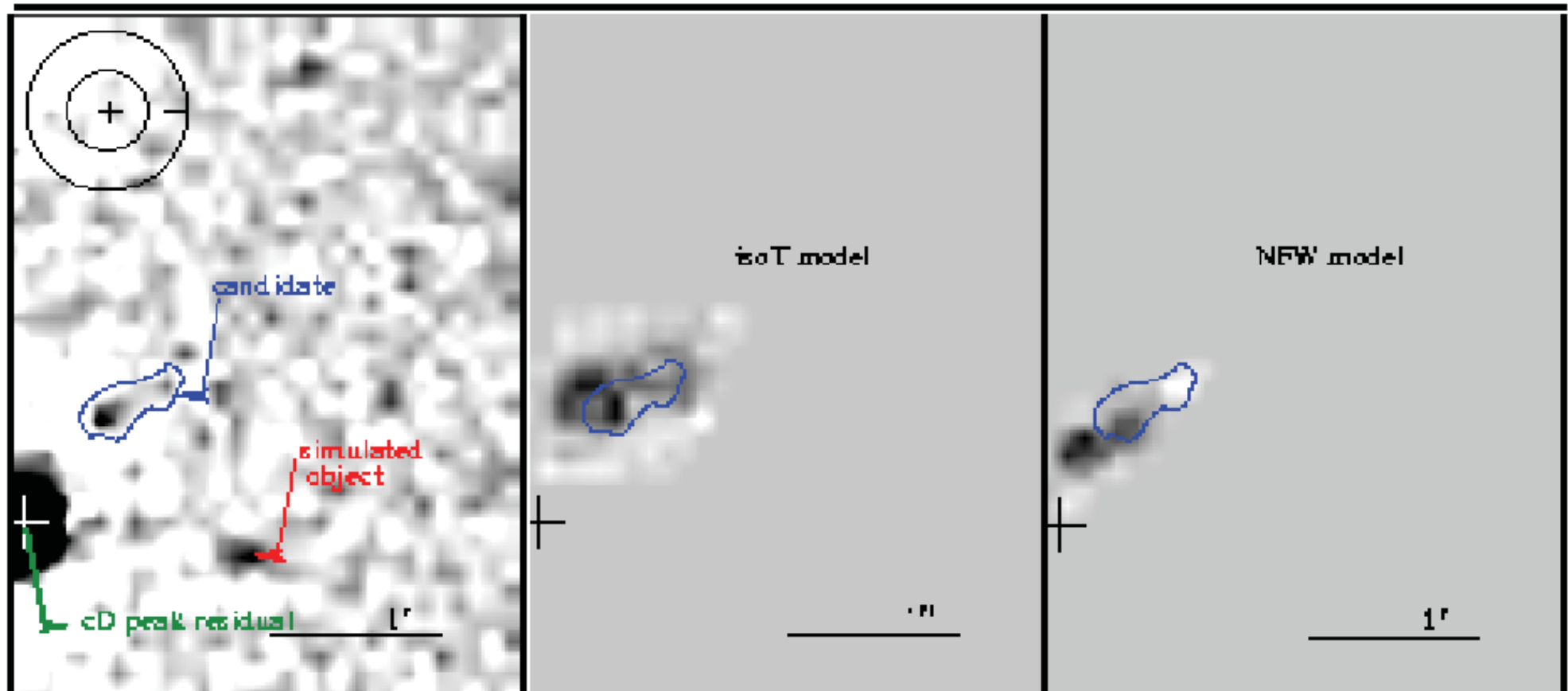


MS2137-23
mass model
 from critical lines
 analysis and 2
 sources



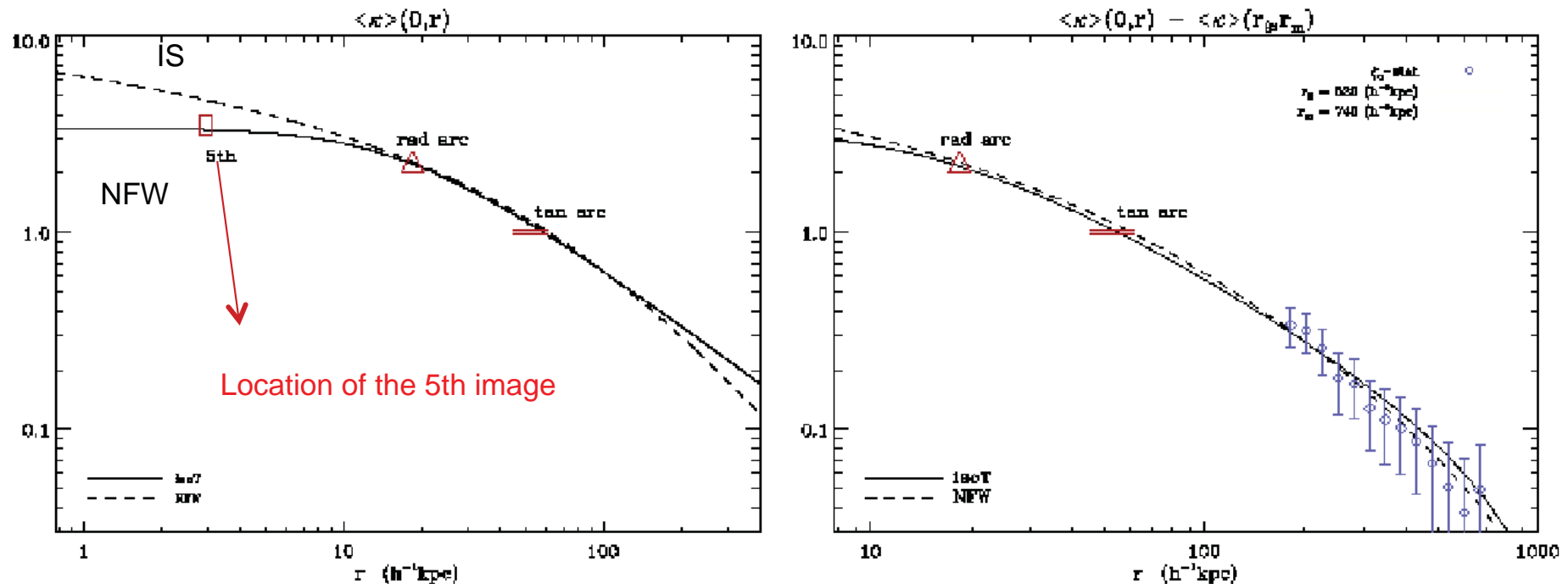
MS2137-23: position and shape of the 5th image: depend on the mass profile

Gavazzi et al 2004



MS2137-23: strong/weak with the 5th image

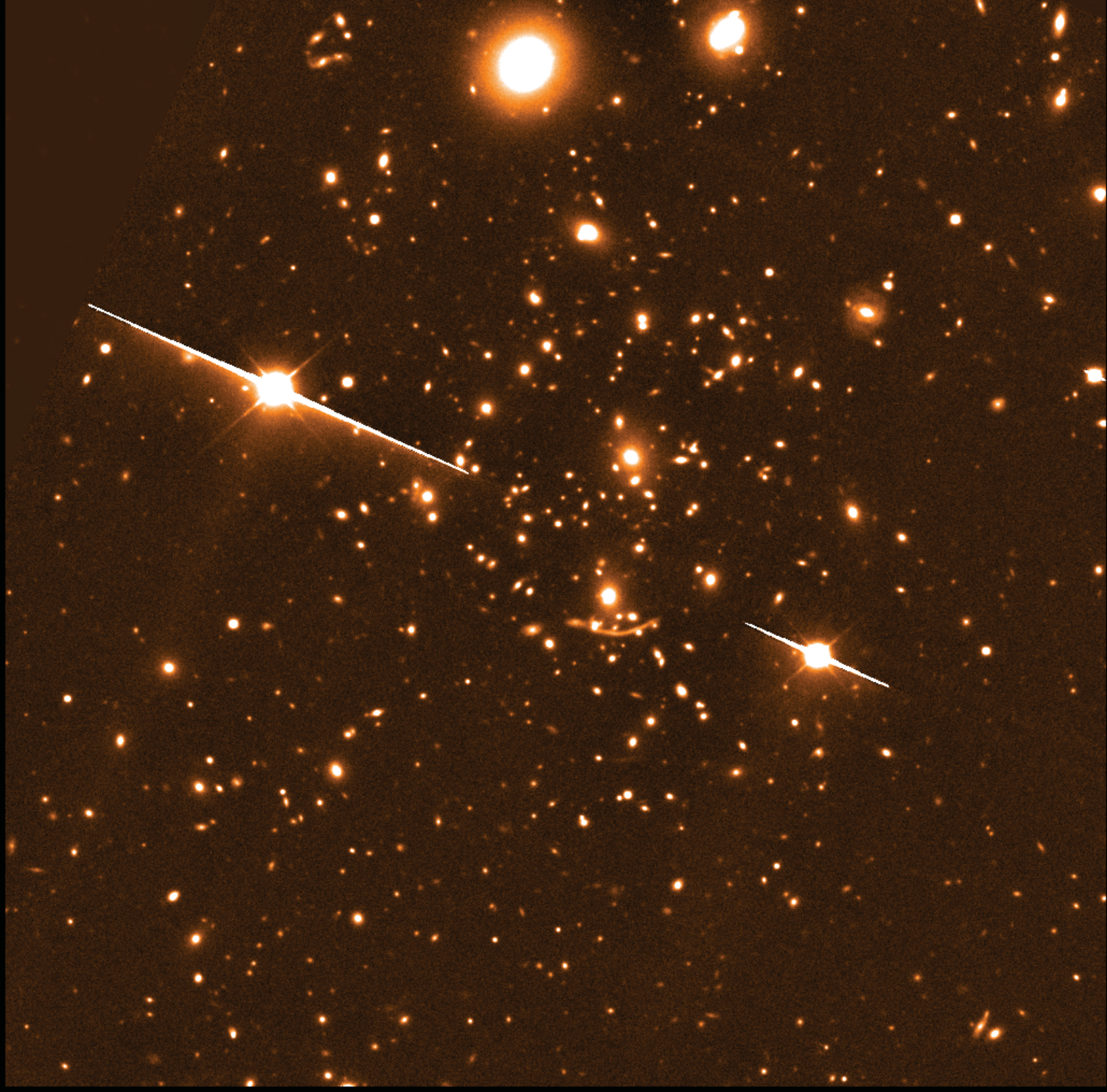
Even a lens configuration with 2 sources and a [radial+tangential] arc system cannot provide conclusive results on SIS vs NFW



Conclusion: find the 5th image!

But not that obvious...if located under a very bright galaxy

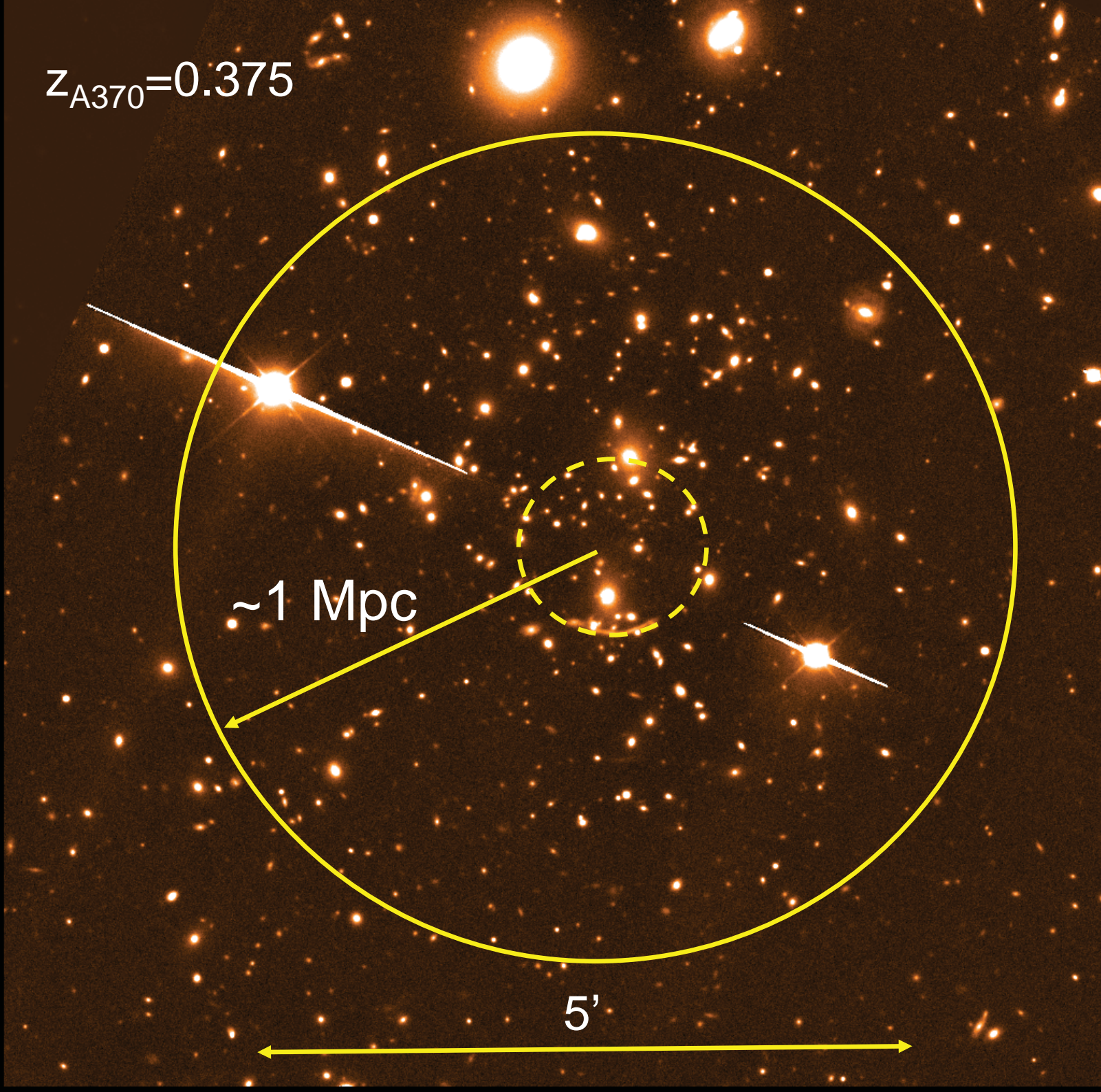
Dark matter with Weak Gravitational Lensing



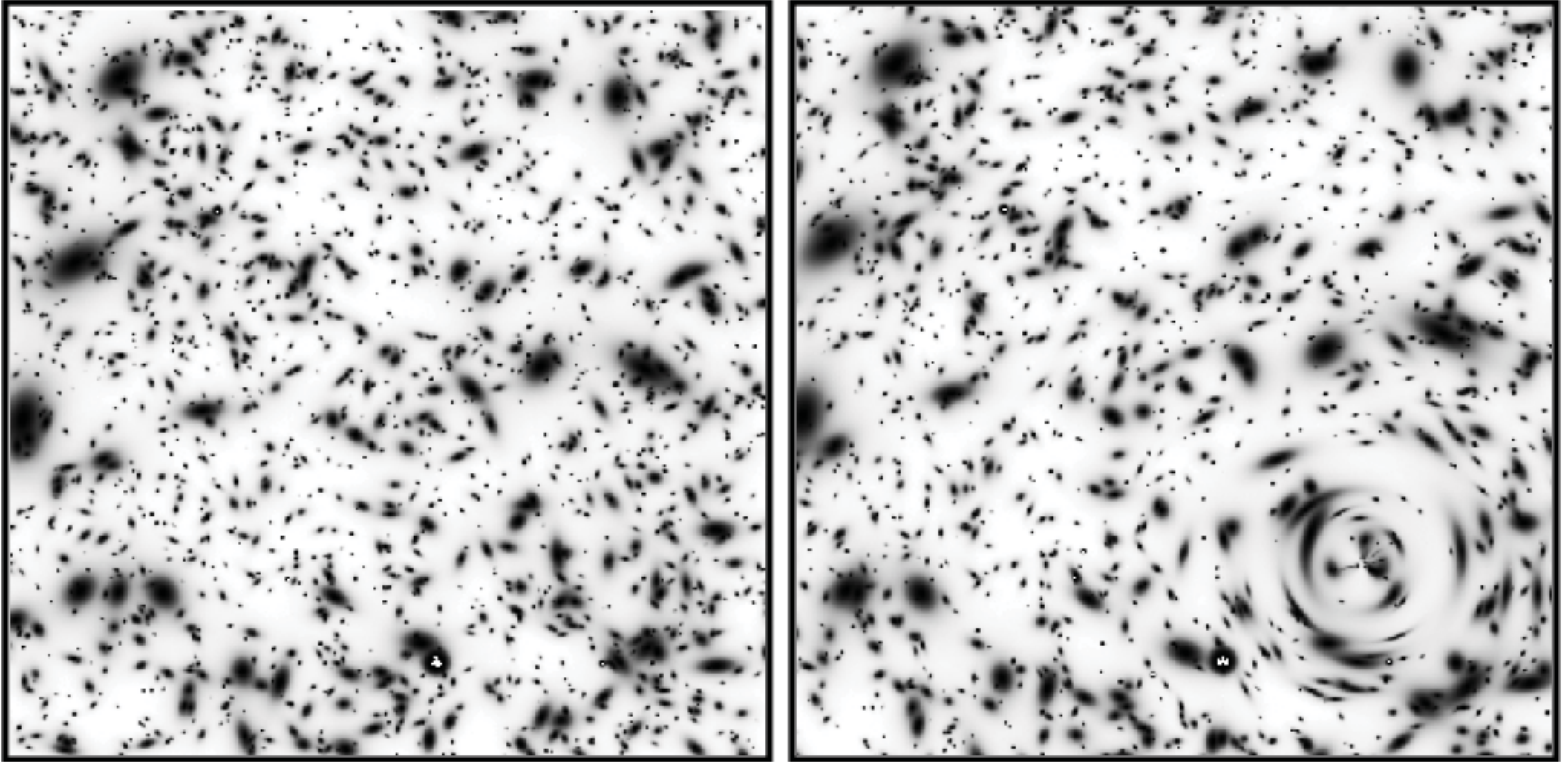
$z_{A370}=0.375$

~ 1 Mpc

5'



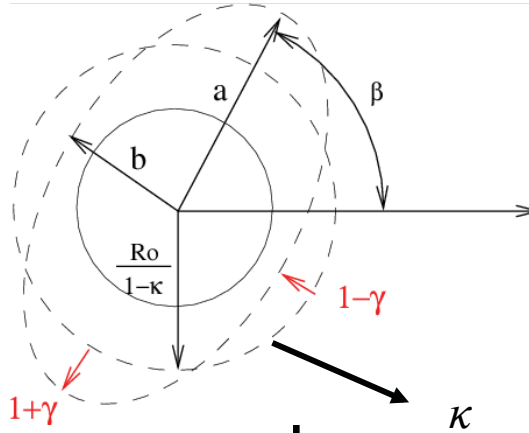
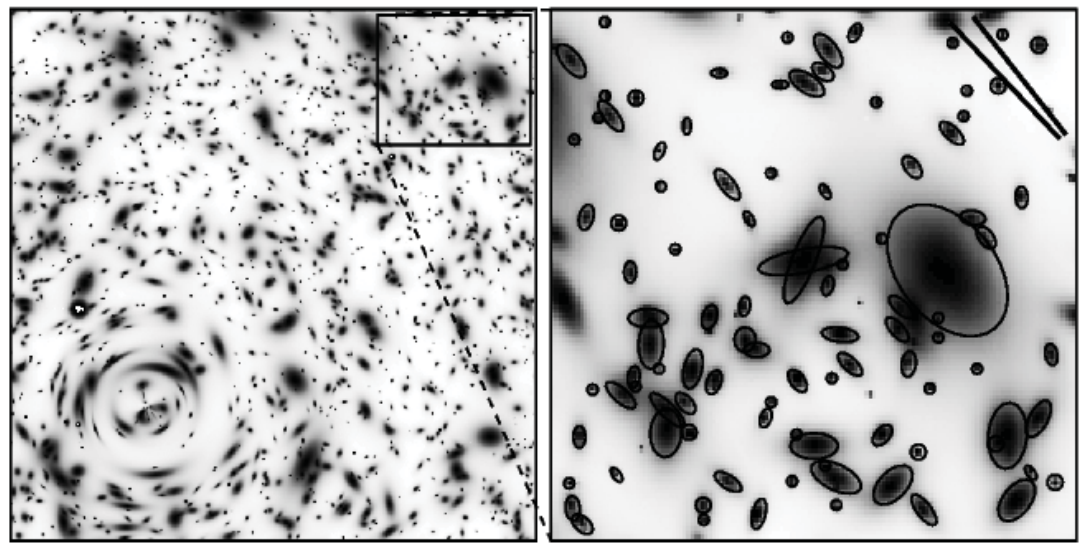
Beyond gravitational arcs: weak lensing



Mellier 1999

Simulation, lensing cluster : isothermal sphere at $z=0.3$

From ellipticity to shear



$$M_{ij} = \frac{\int I(\theta) \theta_i \theta_j d^2\theta}{\int I(\theta) d^2\theta}$$

$$\delta = \frac{2\gamma(1-\kappa)}{(1-\kappa)^2 + |\gamma|^2} = \frac{a^2 - b^2}{a^2 + b^2}$$

$$\frac{a^2 - b^2}{a^2 + b^2}$$

$$\delta \sim 2\gamma \quad (\text{weak lensing regime})$$

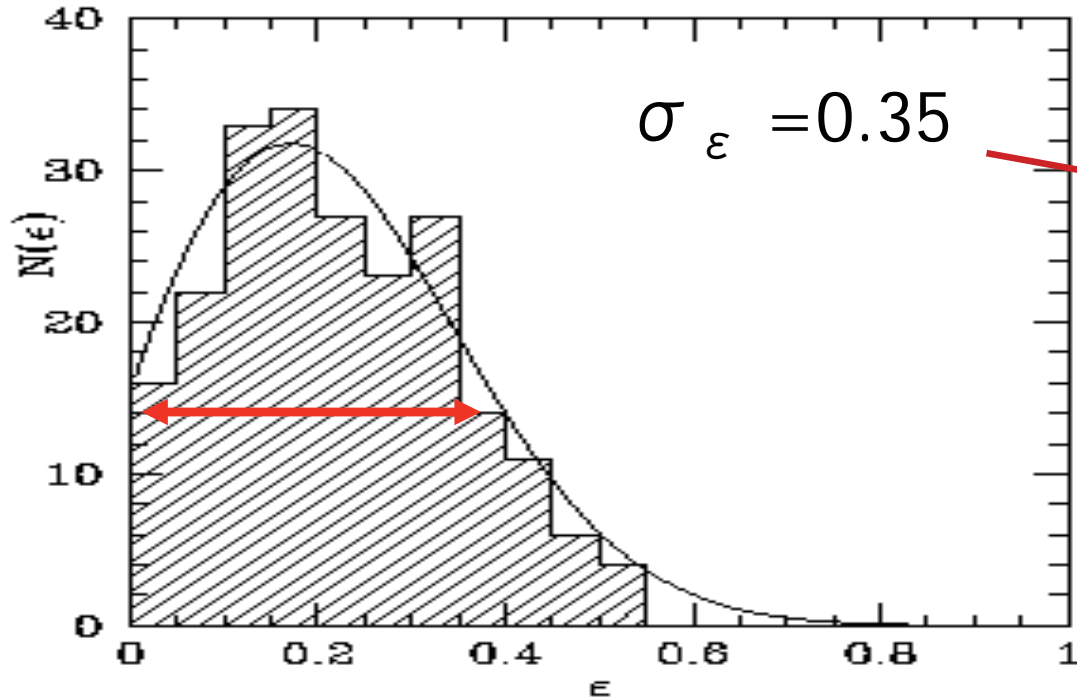
$$= \epsilon_s + \epsilon_i + \text{noise} + \text{systematics} \dots$$

Reliability of results: depends on PSF analysis

Assume sources orientation is isotropic:

Weak lensing regime : $\delta \sim 2\gamma = \langle \epsilon_{\text{Shear}} \rangle_{\theta} + \text{noise} + \text{complications}$

Complication: galaxy ellipticity contaminates gravitational ellipticity



$$E(\epsilon^2) = \sum_{ij} \gamma_t(\theta_i) \gamma_t(\theta_j) + \delta_{ij} \frac{\sigma_\epsilon}{2}$$

$$S/N = 10 \left(\frac{n}{30 \text{ arcmin}^2} \right)^{1/2} \left(\frac{\sigma_\epsilon}{0.2} \right)^{-1} \left(\frac{\sigma_v}{600 \text{ km/s}} \right)^2 \left(\frac{\ln \left[\frac{\theta_2}{\theta_1} \right]}{\ln 10} \right)^{1/2} \left\langle \frac{D_{ls}}{D_{os}} \right\rangle$$

From shear to mass density

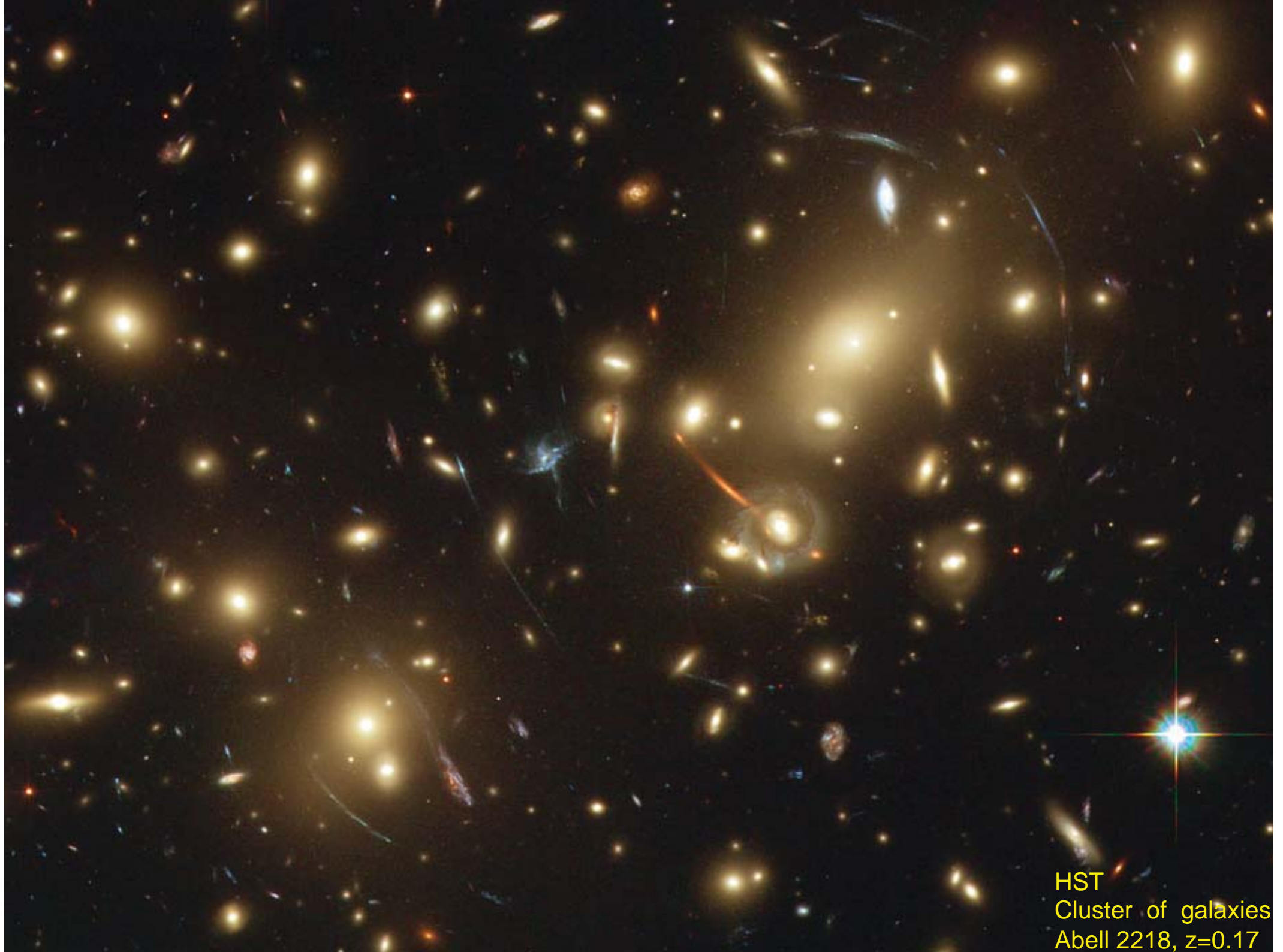
2D mass density map = Distortion (ellipticity) map

$$\kappa(\theta) = \frac{1}{\pi} \int \hat{F}^*(\theta - \theta') \gamma(\theta') d\theta^2 + \kappa_0$$

Application to real data. Sampling ellipticities on a grid:

$$\Sigma(\theta) - \Sigma_0 = \Sigma_{critic} \frac{1}{\pi} a^2 \sum_{i,j} \Re(\hat{F}^*(\theta - \theta_{i,j}) \bar{\epsilon}(\theta_{i,j}))$$

where a is the distance between grid points

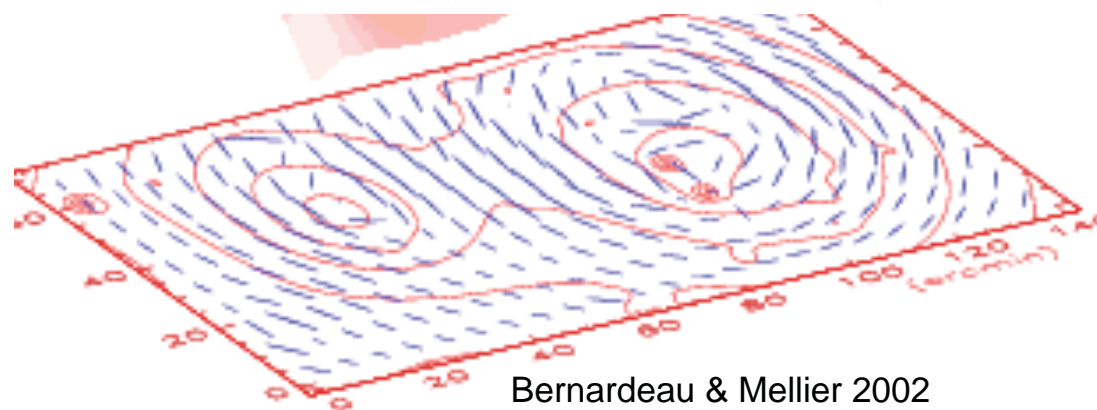
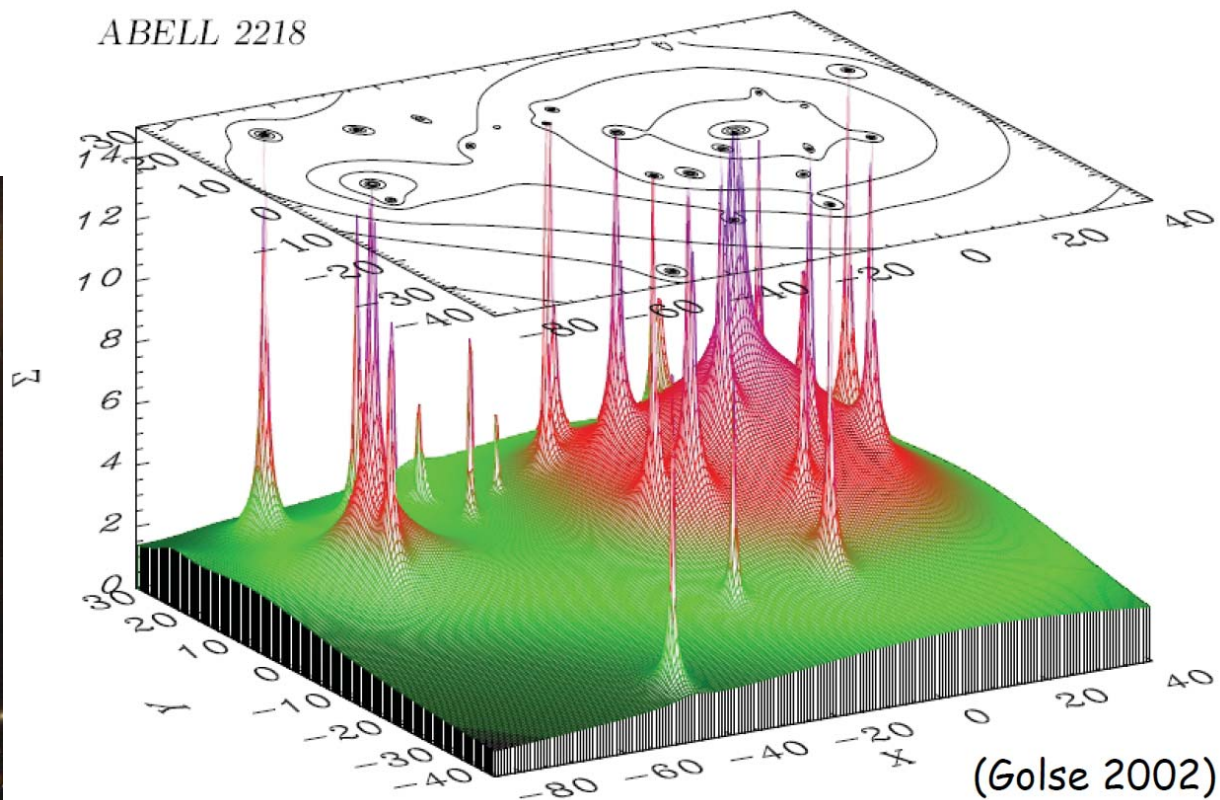


HST
Cluster of galaxies
Abell 2218, $z=0.17$

Mass reconstruction: Abell 2218



ABELL 2218



Bernardeau & Mellier 2002

HST
Abell 1689
Light (galaxies)



Abell 1689
Dark matter

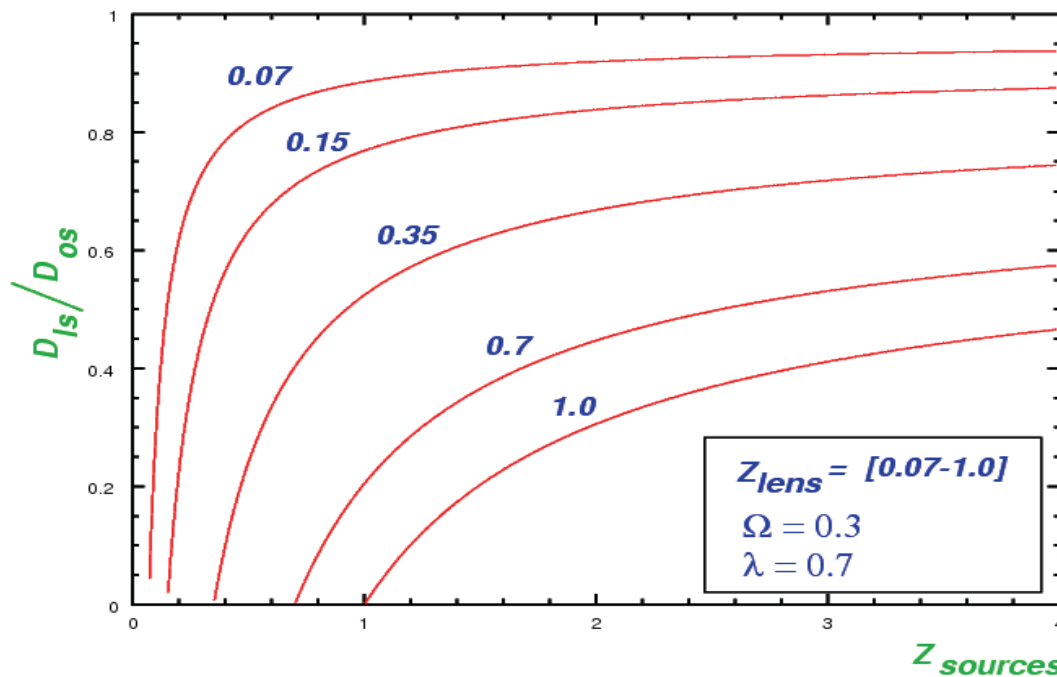


Getting the absolute mass

- The mass reconstruction provides the shape of the projected mass distribution but not the absolute scale.
- Need the redshift of the sources:

$$\kappa(\vec{\theta}, z) = \frac{\Sigma(\vec{\theta})}{\Sigma_{critic}(z)} = \Sigma(\vec{\theta}) \frac{4\pi G}{c^2} D_{ol} \left[\frac{D_{ls}}{D_{os}} \right]$$

$$\gamma(\vec{\theta}, z) = \frac{4\pi G}{c^2} D_{ol} \left[\frac{D_{ls}}{D_{os}} \right] \gamma(\vec{\theta})$$

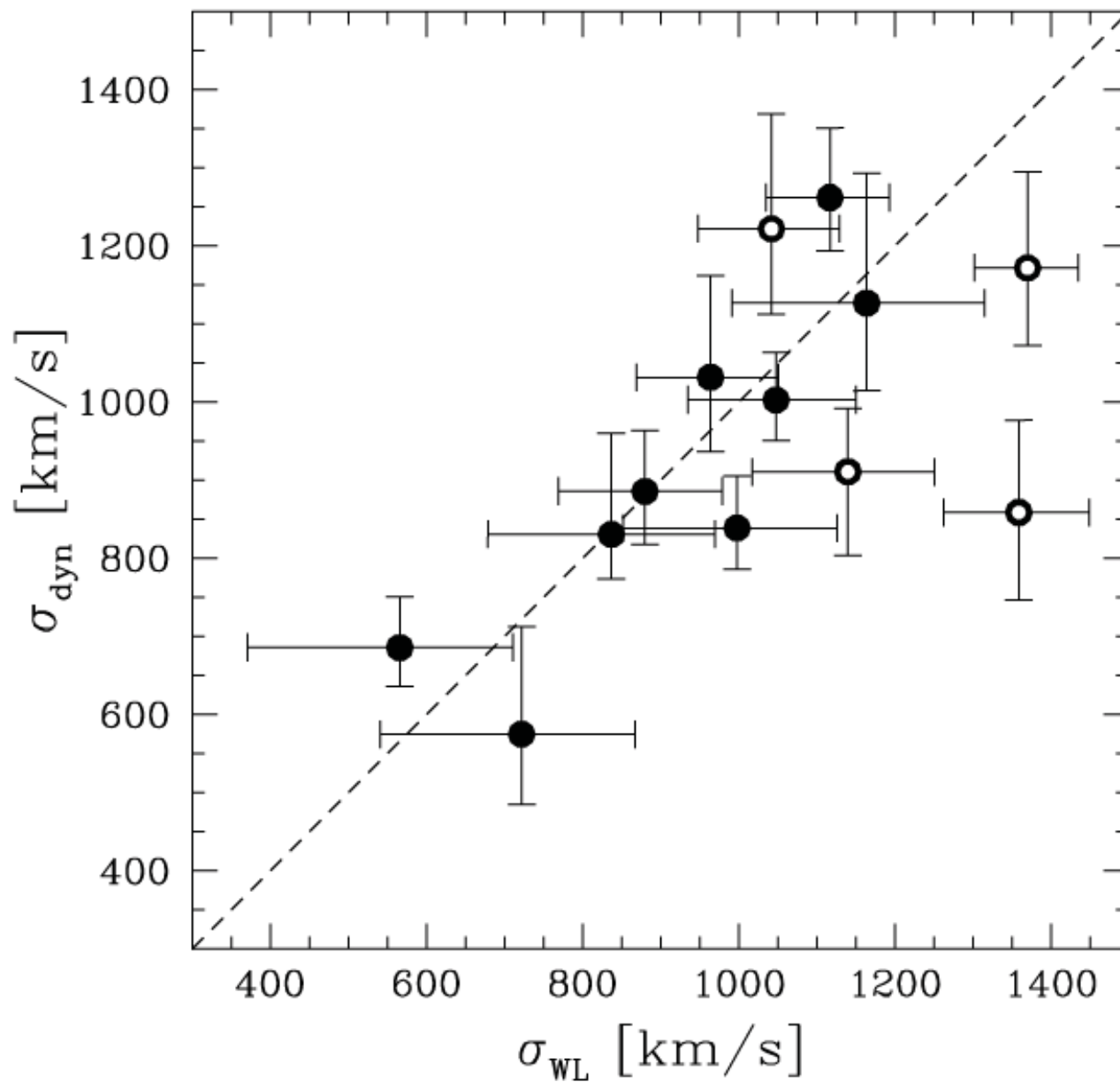


Redshift increasingly important as z_{lens} increases

Summary mass from cluster WL reconstruction

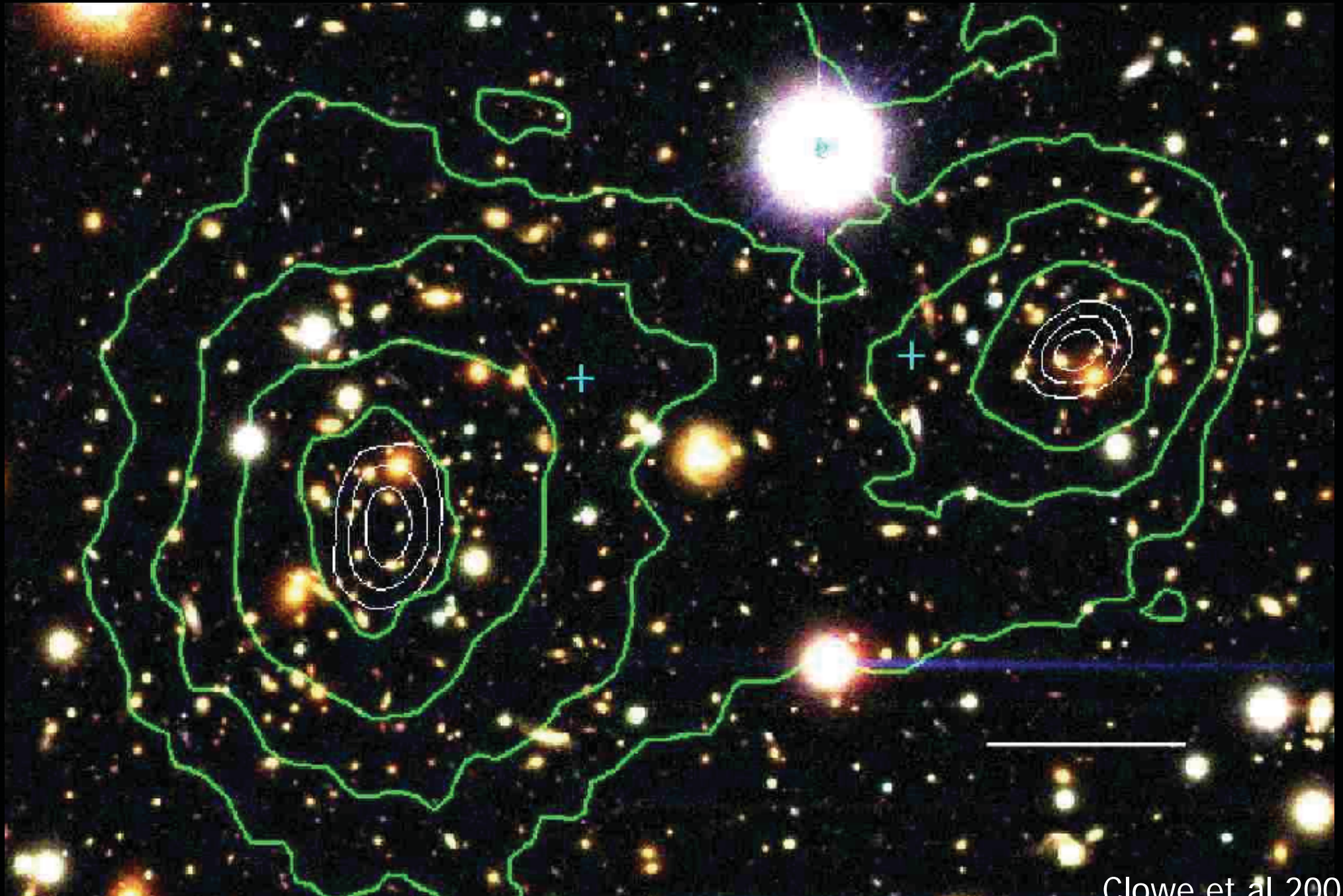
| (1) Name | (2) σ_{WL} (km s ⁻¹) SIS | (3) $M(<0.5h^{-1} \text{ Mpc})$ WL by aperture mass | (4) M_{2500} | (5) M_{500} | (6) M_{2500}^{NFW} | (7) M_{500}^{NFW} | (8) M_{200}^{NFW} |
|-------------|--|---|-------------------|---|-------------------------------------|--------------------------------------|--------------------------------------|
| | | | | WL using NFW profile fitting of the shear | | | |
| A2390 | 1117 ⁺⁷⁶ ₋₈₂ | 5.2 ± 0.6 | 2.4 ± 0.5 | 6.8 ± 1.5 | 2.9 ± 0.6 | 9.2 ^{+2.0} _{-1.9} | 14.6 ^{+3.1} _{-2.9} |
| MS 0016+16 | 1164 ⁺¹⁵¹ ₋₁₇₃ | 7.9 ± 1.1 | 3.2 ± 0.7 | 15.8 ± 4.3 | 4.2 ^{+1.4} _{-1.3} | 16.0 ^{+5.3} _{-4.9} | 27.0 ^{+9.0} _{-8.4} |
| MS 0906+11 | 880 ⁺⁹⁹ ₋₁₁₁ | 3.7 ± 0.7 | 1.6 ± 0.4 | 7.4 ± 1.5 | 1.5 ± 0.4 | 4.4 ^{+1.2} _{-0.2} | 6.7 ^{+1.8} _{-1.8} |
| MS 1224+20 | 837 ⁺¹³³ ₋₁₅₈ | 3.0 ± 0.9 | 1.0 ± 0.4 | 2.3 ± 1.2 | 0.8 ± 0.4 | 2.1 ^{+1.2} _{-1.0} | 3.2 ^{+1.8} _{-1.5} |
| MS 1231+15 | 566 ⁺¹⁴⁵ ₋₁₉₅ | 0.8 ± 0.6 | 0.4 ± 0.2 | 0.5 ± 0.5 | 0.4 ± 0.2 | 0.9 ^{+0.5} _{-0.5} | 1.3 ^{+0.7} _{-0.7} |
| MS 1358+62 | 1048 ⁺¹⁰² ₋₁₁₃ | 4.3 ± 0.8 | 1.8 ± 0.4 | 5.6 ± 2.0 | 1.8 ^{+0.6} _{-0.5} | 5.5 ^{+1.9} _{-1.7} | 8.5 ^{+3.0} _{-2.6} |
| MS 1455+22 | 964 ⁺⁸⁷ ₋₉₅ | 3.3 ± 0.7 | 1.2 ± 0.3 | 3.7 ± 1.2 | 1.4 ^{+0.4} _{-0.3} | 3.9 ^{+1.0} _{-1.0} | 6.0 ^{+1.6} _{-1.5} |
| MS 1512+36 | 722 ⁺¹⁴⁵ ₋₁₈₁ | 2.1 ± 0.8 | 0.6 ± 0.3 | 2.5 ± 1.6 | 0.7 ^{+0.4} _{-0.3} | 1.8 ^{+1.1} _{-0.9} | 2.8 ^{+1.6} _{-1.4} |
| MS 1621+26 | 998 ⁺¹²⁸ ₋₁₄₆ | 5.3 ± 1.0 | 1.7 ± 0.7 | 5.8 ± 2.0 | 2.0 ^{+0.8} _{-0.6} | 6.5 ^{+2.8} _{-1.9} | 10.3 ^{+4.4} _{-3.0} |
| A68 | 1036 ⁺⁸⁹ ₋₉₇ | 4.4 ± 0.8 | 1.9 ± 0.4 | 4.8 ± 1.8 | 1.8 ^{+0.5} _{-0.4} | 5.6 ^{+1.6} _{-1.3} | 8.6 ^{+2.5} _{-2.1} |
| A209 | 898 ⁺⁹² ₋₁₀₂ | 3.9 ± 0.9 | 1.5 ± 0.6 | 5.7 ± 1.4 | 1.5 ^{+0.5} _{-0.4} | 4.3 ^{+1.4} _{-1.1} | 6.6 ^{+2.1} _{-1.7} |
| A267 | 1008 ⁺⁹⁰ ₋₉₉ | 3.3 ± 0.6 | 1.5 ± 0.3 | 4.3 ± 1.4 | 1.4 ± 0.4 | 4.0 ^{+1.2} _{-1.2} | 6.2 ^{+1.9} _{-1.8} |
| A383 | 701 ⁺¹³⁸ ₋₁₇₁ | 2.6 ± 0.7 | 0.6 ± 0.3 | 3.7 ± 1.6 | 0.6 ^{+0.4} _{-0.3} | 1.6 ^{+0.9} _{-0.8} | 2.3 ^{+1.3} _{-1.2} |
| A963 | 844 ⁺⁹⁹ ₋₁₁₂ | 2.7 ± 0.6 | 1.0 ± 0.3 | 3.1 ± 1.1 | 1.3 ± 0.4 | 3.5 ^{+1.1} _{-1.0} | 5.3 ^{+1.6} _{-1.5} |
| A1689 | 1370 ⁺⁶⁵ ₋₆₈ | 6.7 ± 0.7 | 3.7 ± 0.5 | 11.2 ± 1.8 | 4.0 ^{+0.8} _{-0.7} | 12.8 ^{+2.7} _{-2.3} | 20.4 ^{+4.2} _{-3.6} |
| A1763 | 1060 ⁺⁸⁷ ₋₉₅ | 4.9 ± 0.7 | 2.3 ± 0.4 | 8.5 ± 2.2 | 2.3 ± 0.6 | 7.0 ^{+2.0} _{-1.7} | 11.0 ^{+3.0} _{-2.7} |
| A2218 | 1042 ⁺⁸⁷ ₋₉₄ | 4.5 ± 0.7 | 2.0 ± 0.5 | 4.6 ± 1.2 | 1.6 ^{+0.5} _{-0.4} | 4.7 ^{+1.5} _{-1.3} | 7.1 ^{+2.3} _{-1.9} |
| A2219 | 1074 ⁺⁸² ₋₈₉ | 5.0 ± 0.7 | 2.3 ± 0.4 | 7.7 ± 1.7 | 2.0 ^{+0.6} _{-0.5} | 5.9 ^{+1.7} _{-1.4} | 9.2 ^{+2.7} _{-2.2} |
| A370 | 1359 ⁺⁹⁰ ₋₉₆ | 6.5 ± 0.9 | 3.1 ± 0.5 | 10.6 ± 2.5 | 3.7 ^{+1.1} _{-0.9} | 12.9 ^{+3.8} _{-3.2} | 21.1 ^{+6.2} _{-5.3} |
| CL0024+16 | 1140 ⁺¹¹¹ ₋₁₂₃ | 5.5 ± 0.9 | 2.3 ± 0.5 | 7.4 ± 2.4 | 2.7 ^{+0.9} _{-0.8} | 9.1 ^{+3.2} _{-2.7} | 14.7 ^{+5.1} _{-4.4} |

Summary mass from cluster WL reconstruction

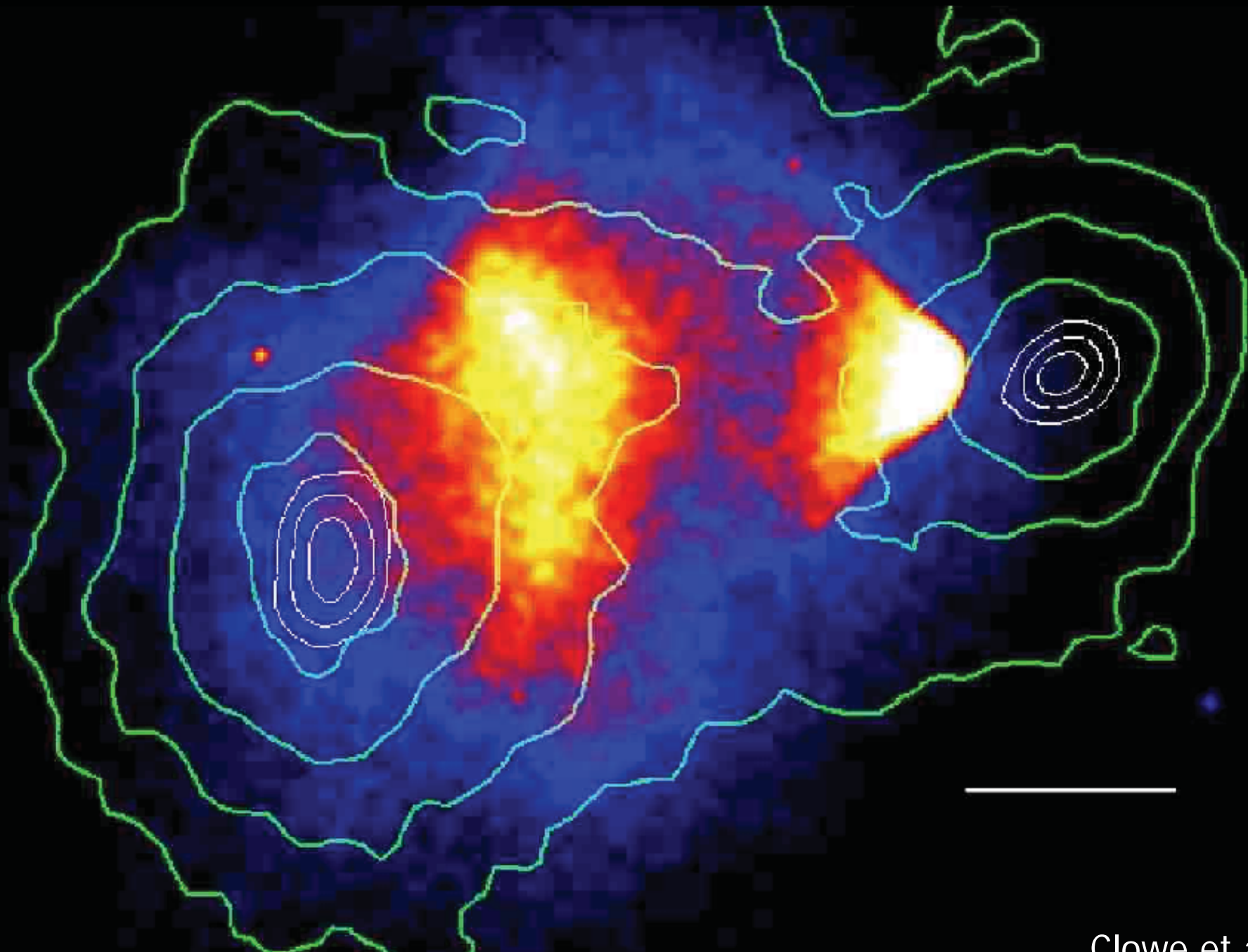


The Bullet cluster

Bullet cluster

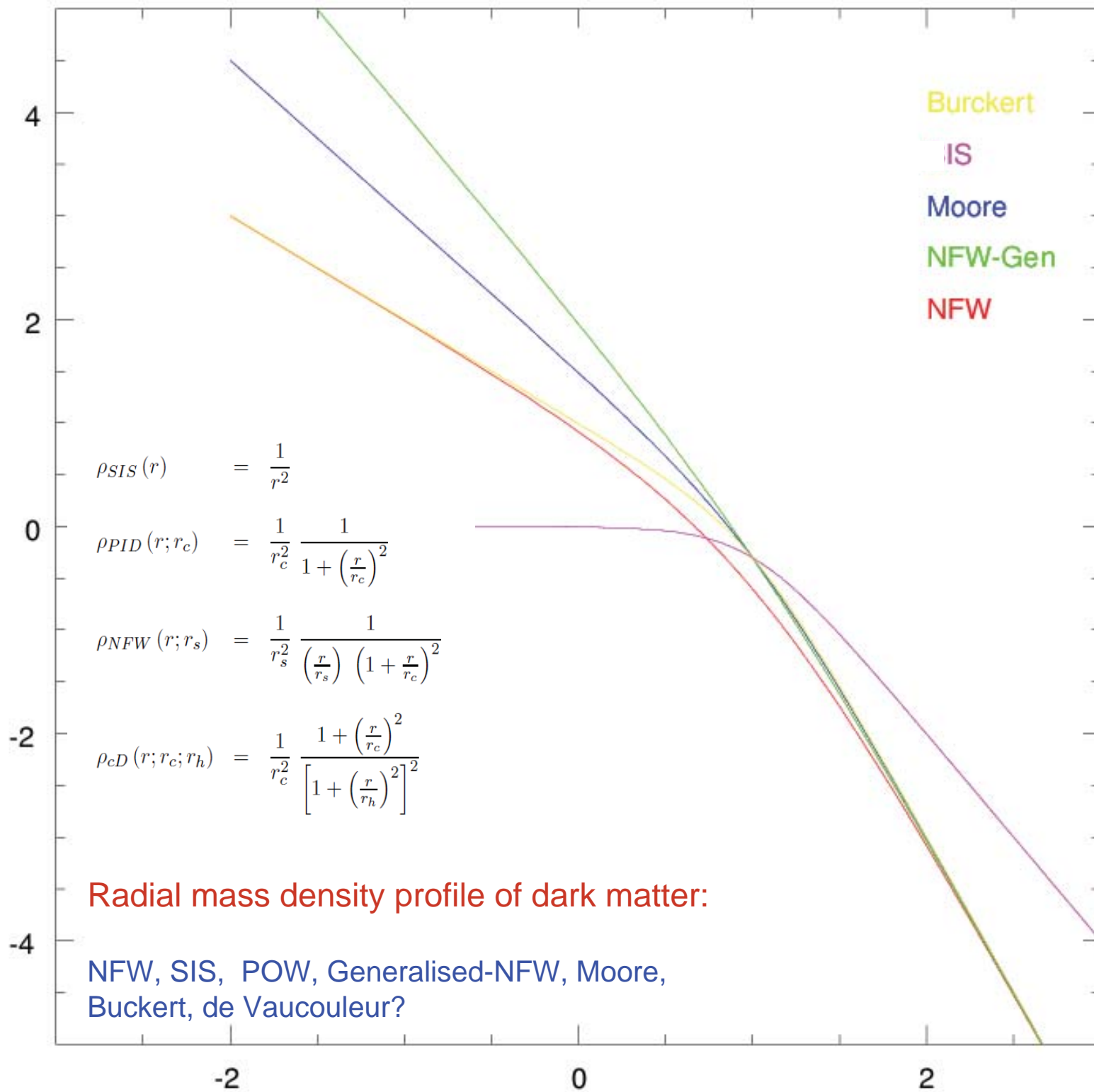


Bullet cluster



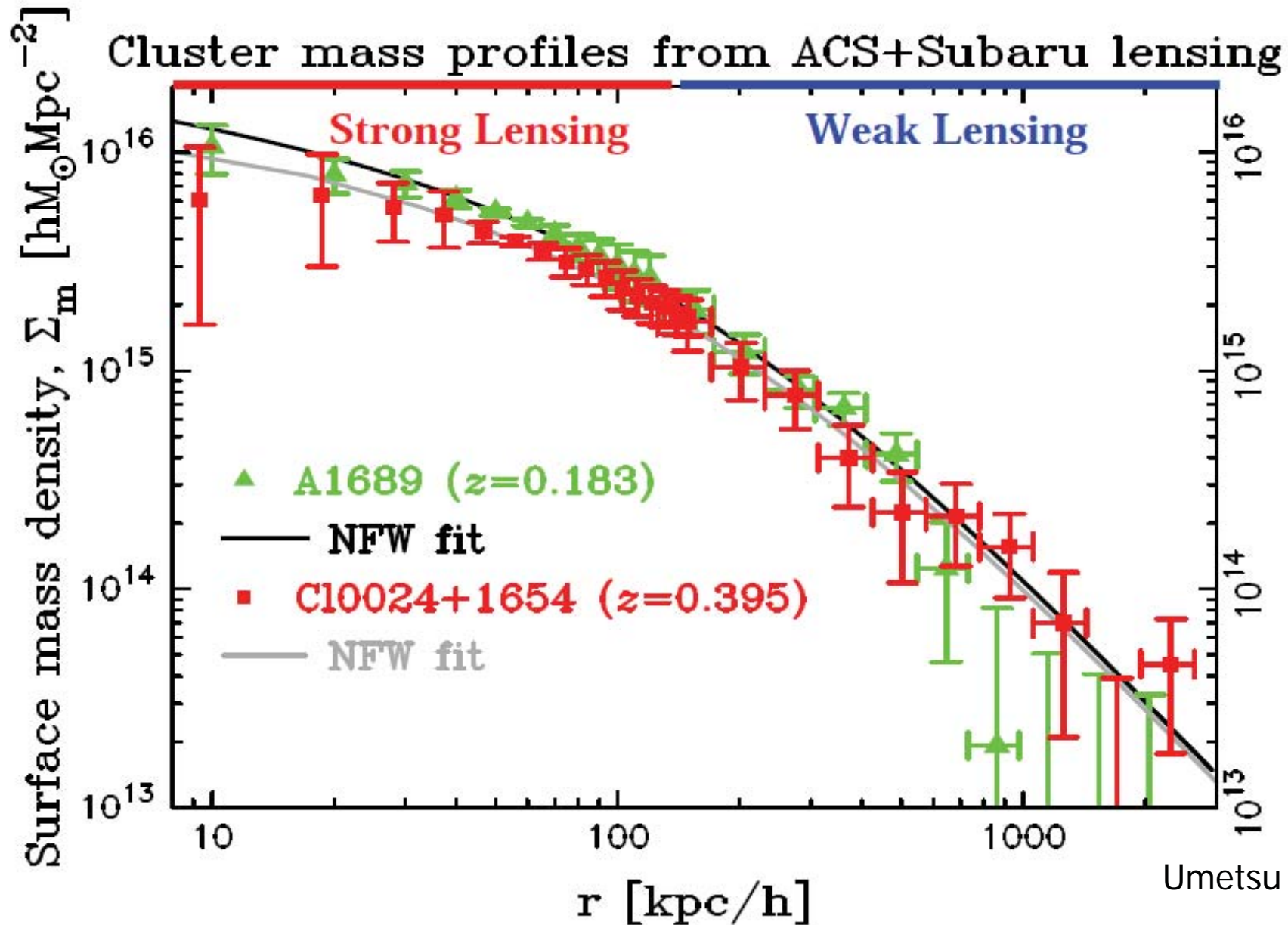
Mass reconstruction

**Application to clusters of
galaxies**

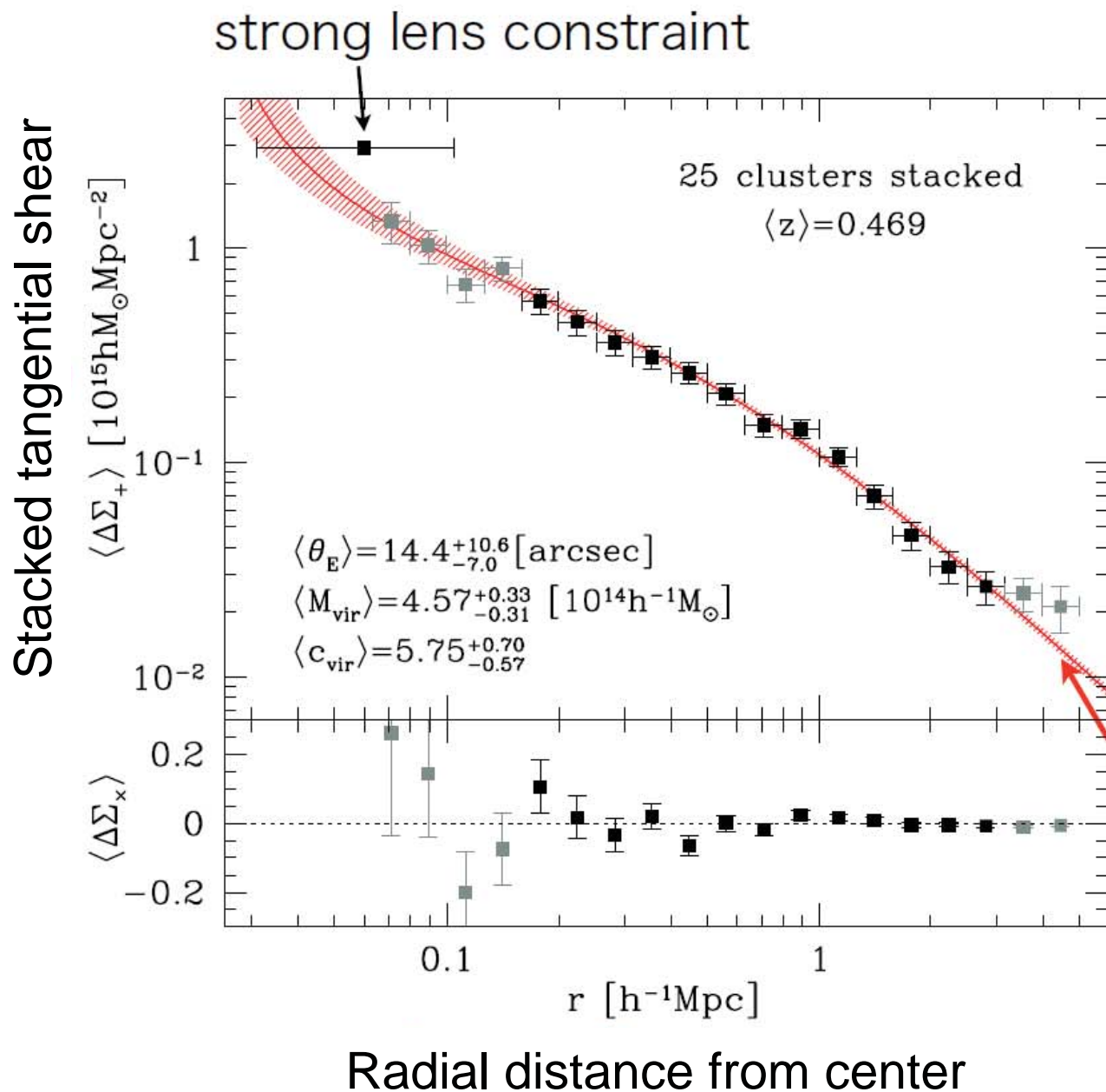


Cl0024+1654 + Abell 1689

Weak+strong lensing



Stacking 25 lensing clusters

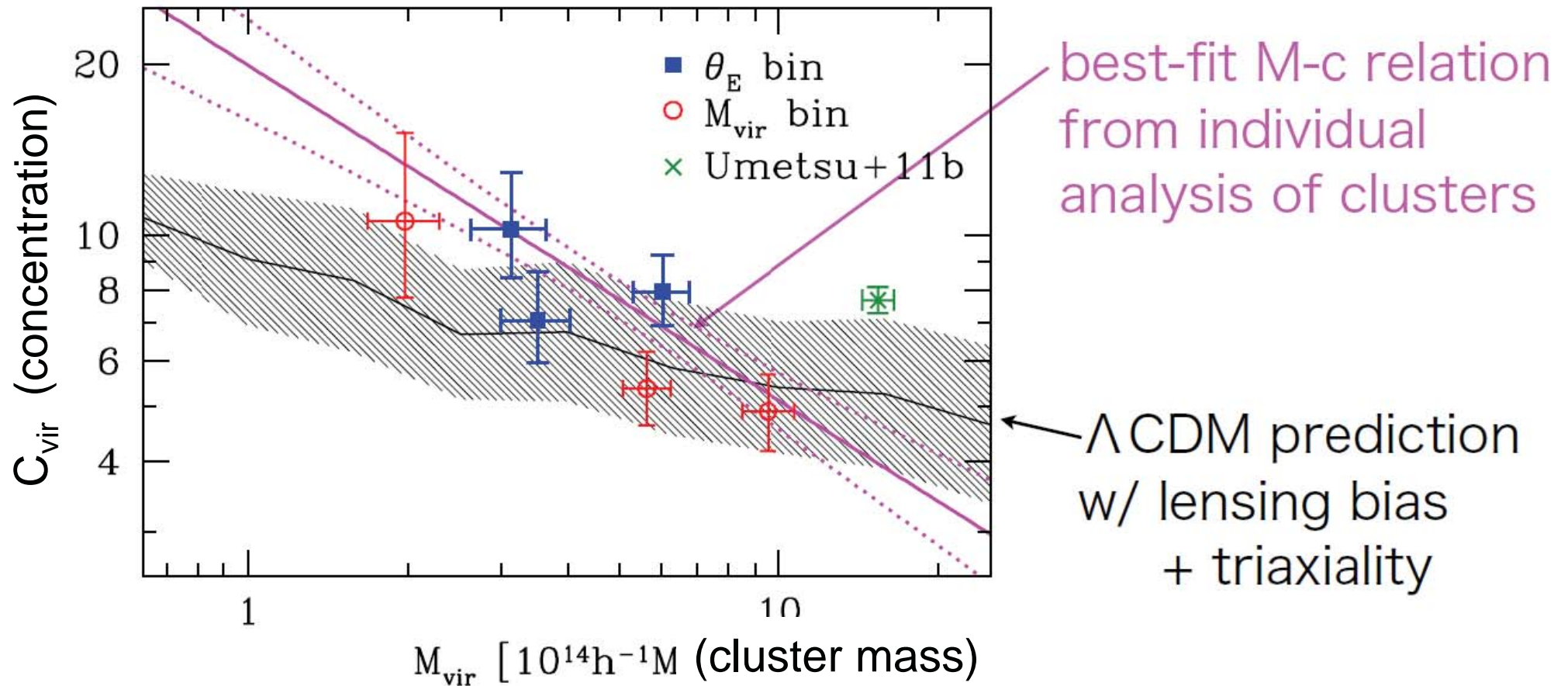


- high S/N lensing shear profile by stacking 25 clusters

- follow NFW well

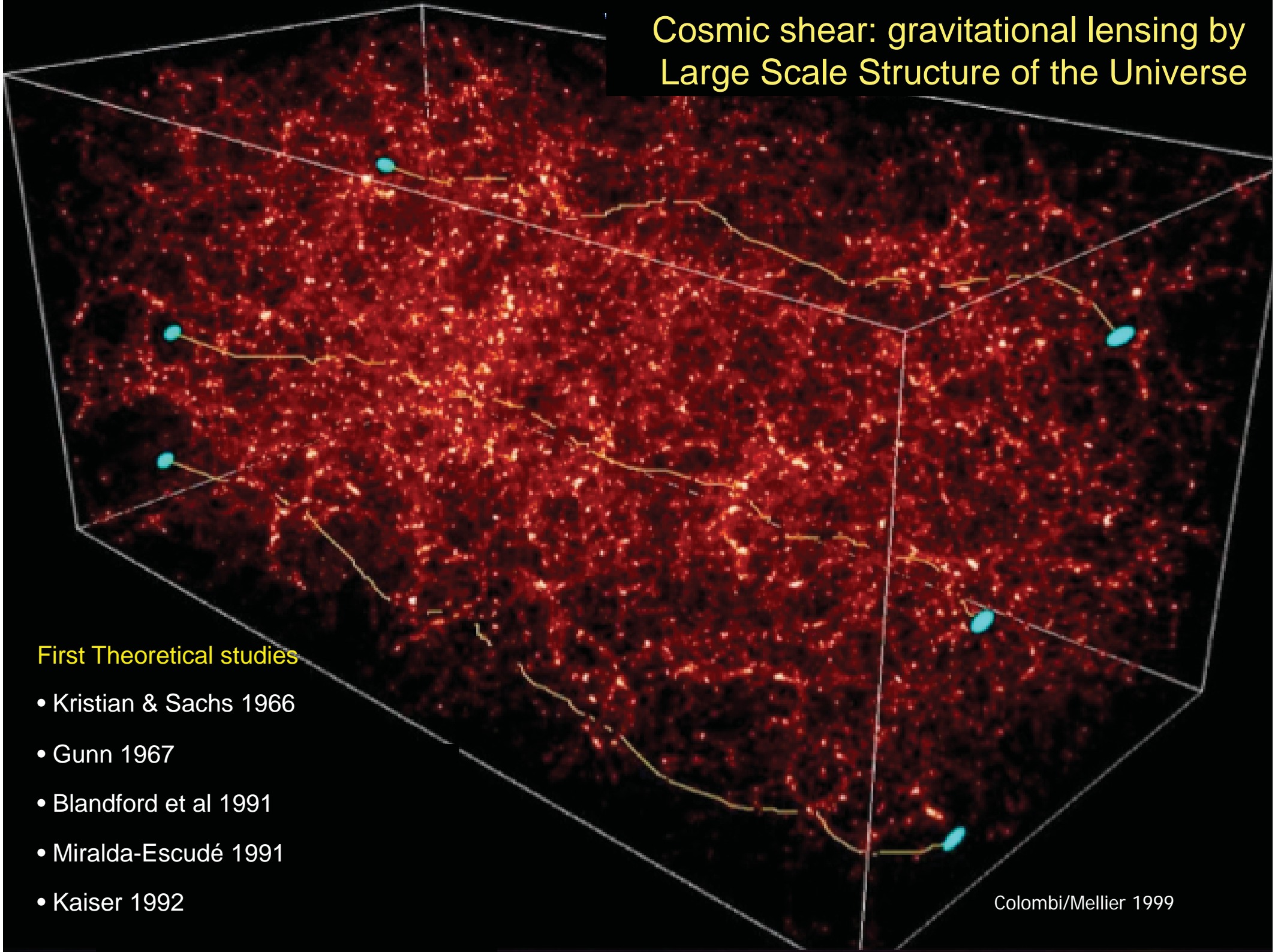
NFW fit

Stacking lensing clusters



Gravitational lensing by large scale structure: cosmic shear

Cosmic shear: gravitational lensing by Large Scale Structure of the Universe



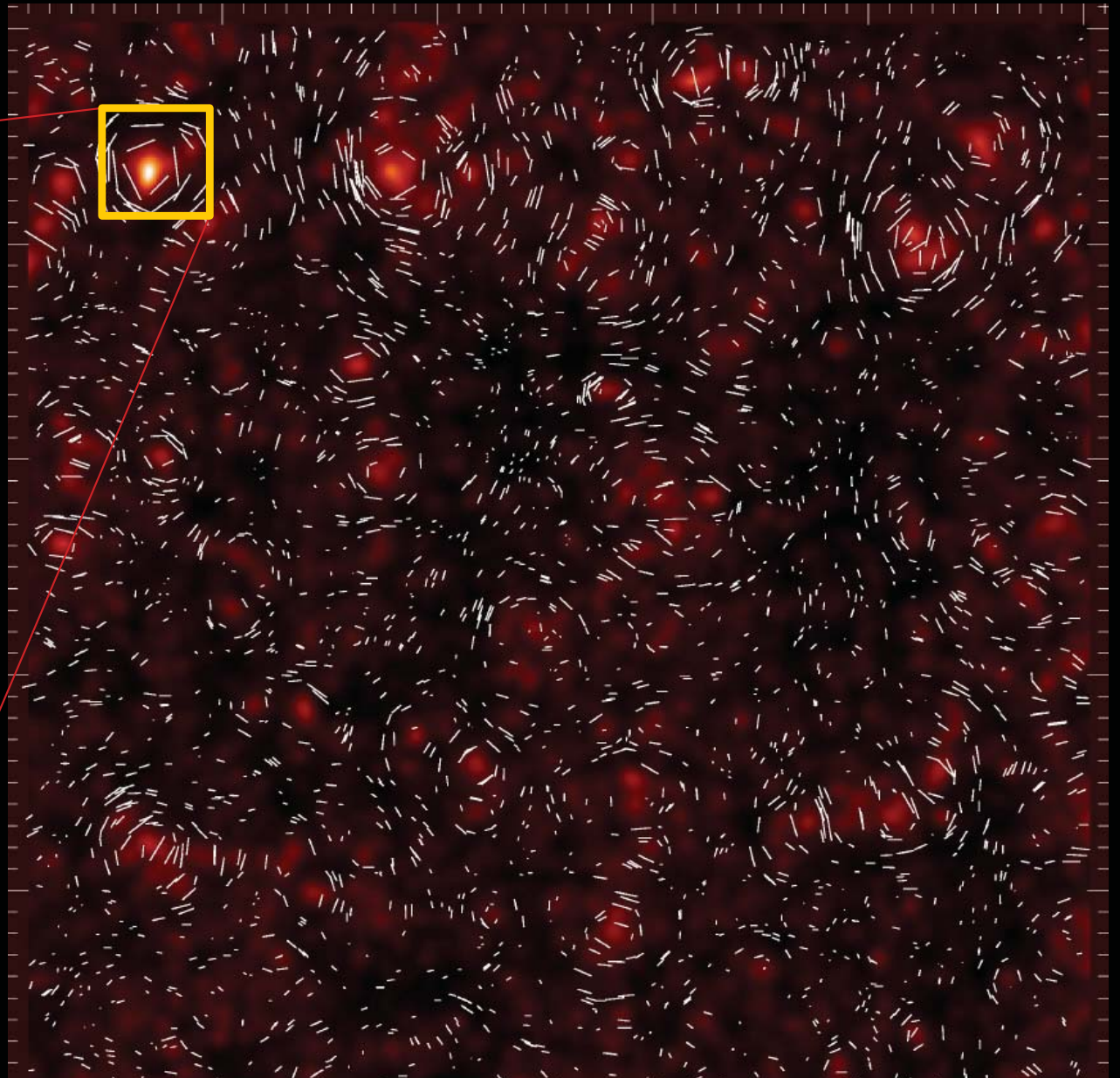
First Theoretical studies

- Kristian & Sachs 1966
- Gunn 1967
- Blandford et al 1991
- Miralda-Escudé 1991
- Kaiser 1992

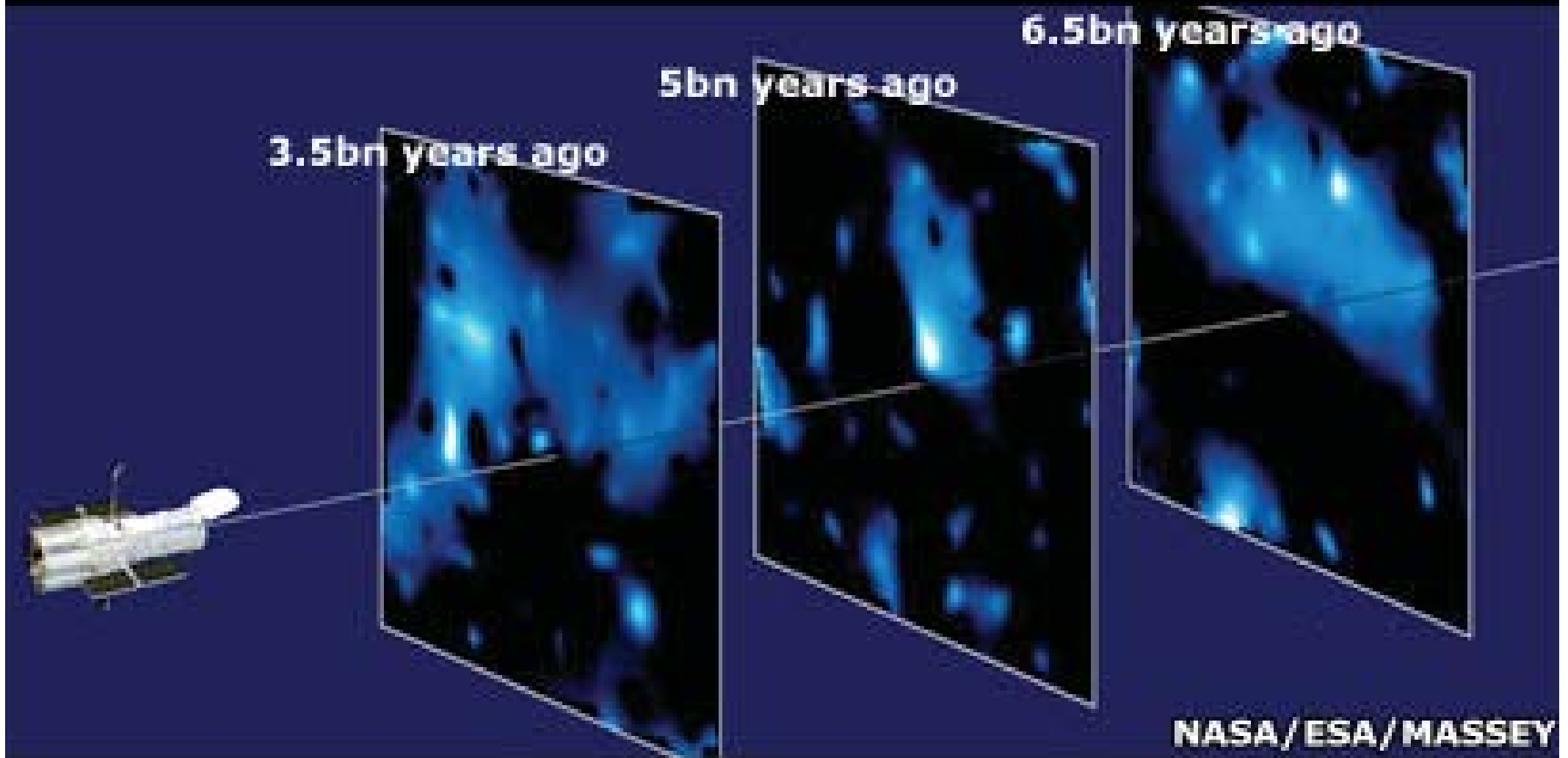
Colombi/Mellier 1999

Cosmic shear: weak gravitational distortion

→ Projected on the sky: coherent ellipticity field



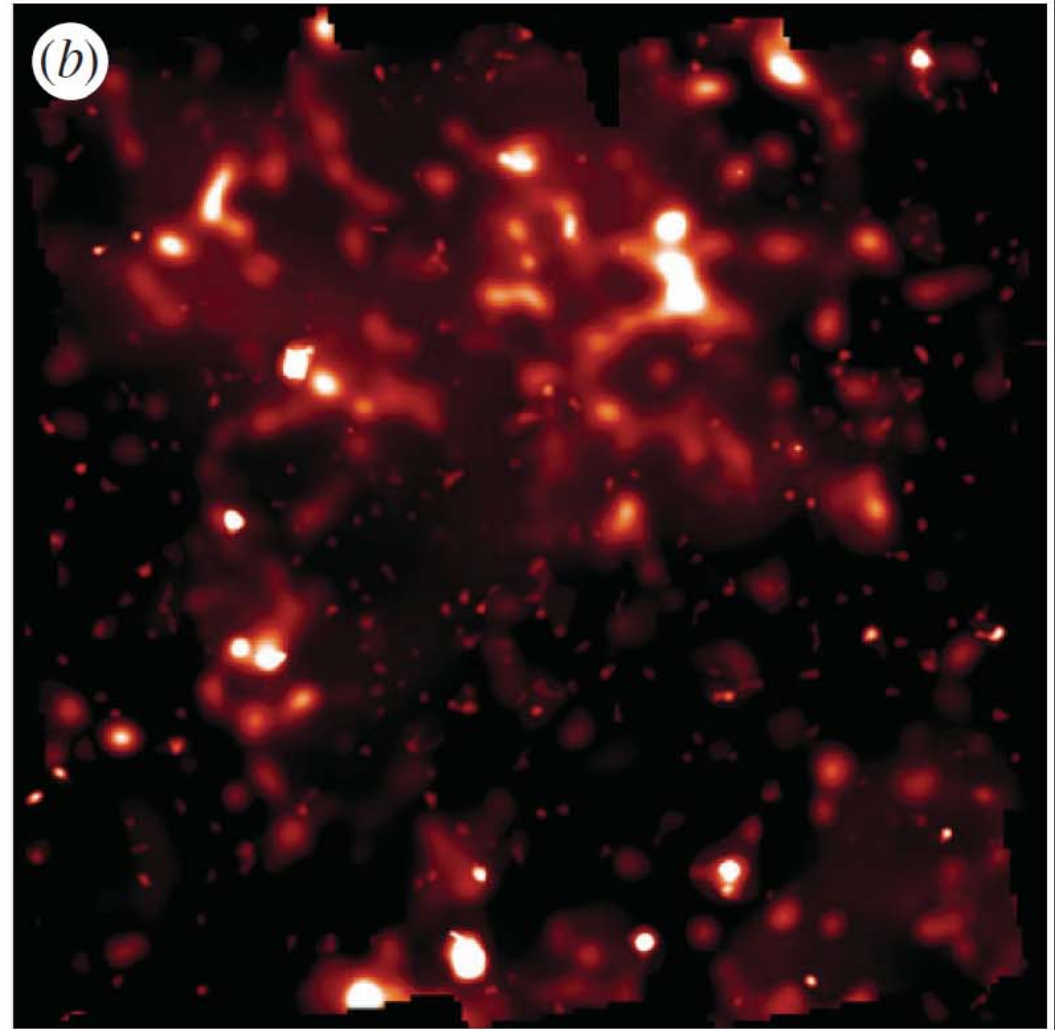
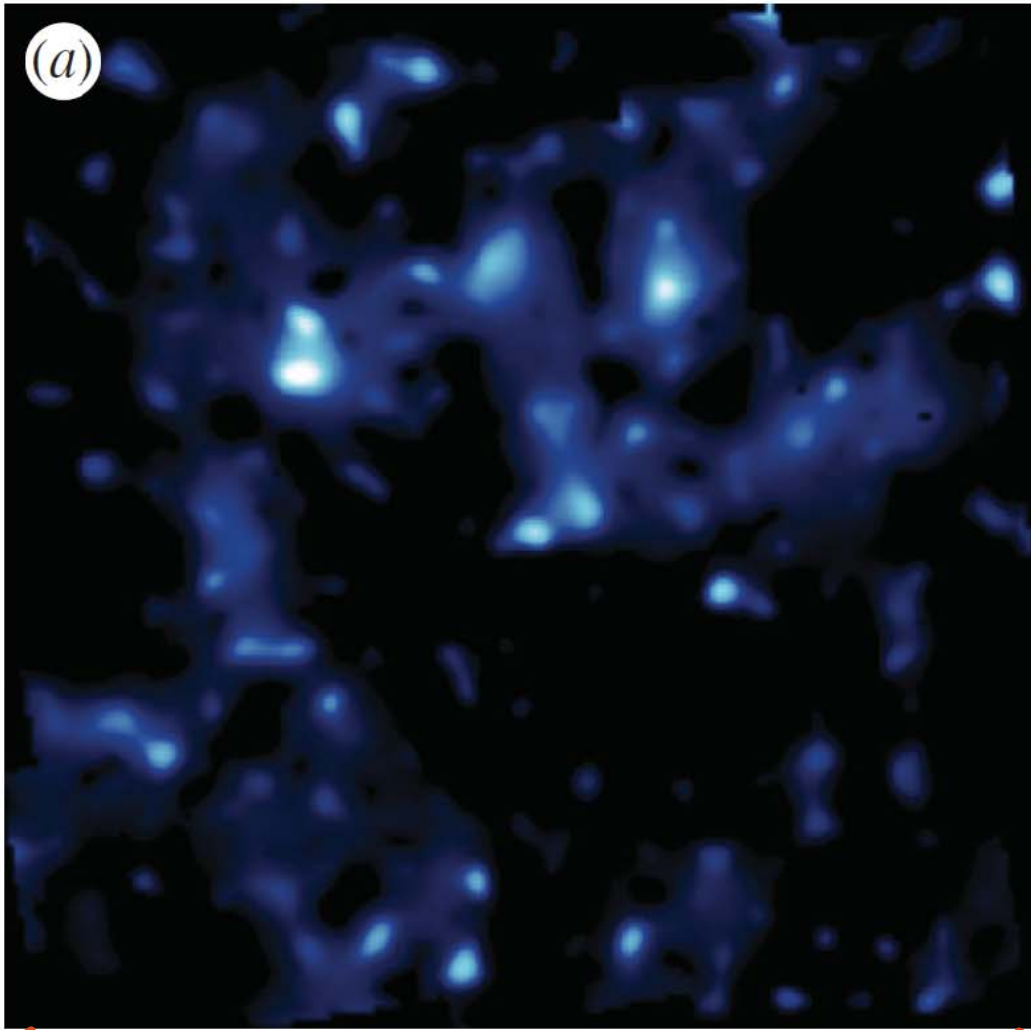
Most spectacular Cosmic shear and tomography with HST



Cosmic shear and tomography with HST

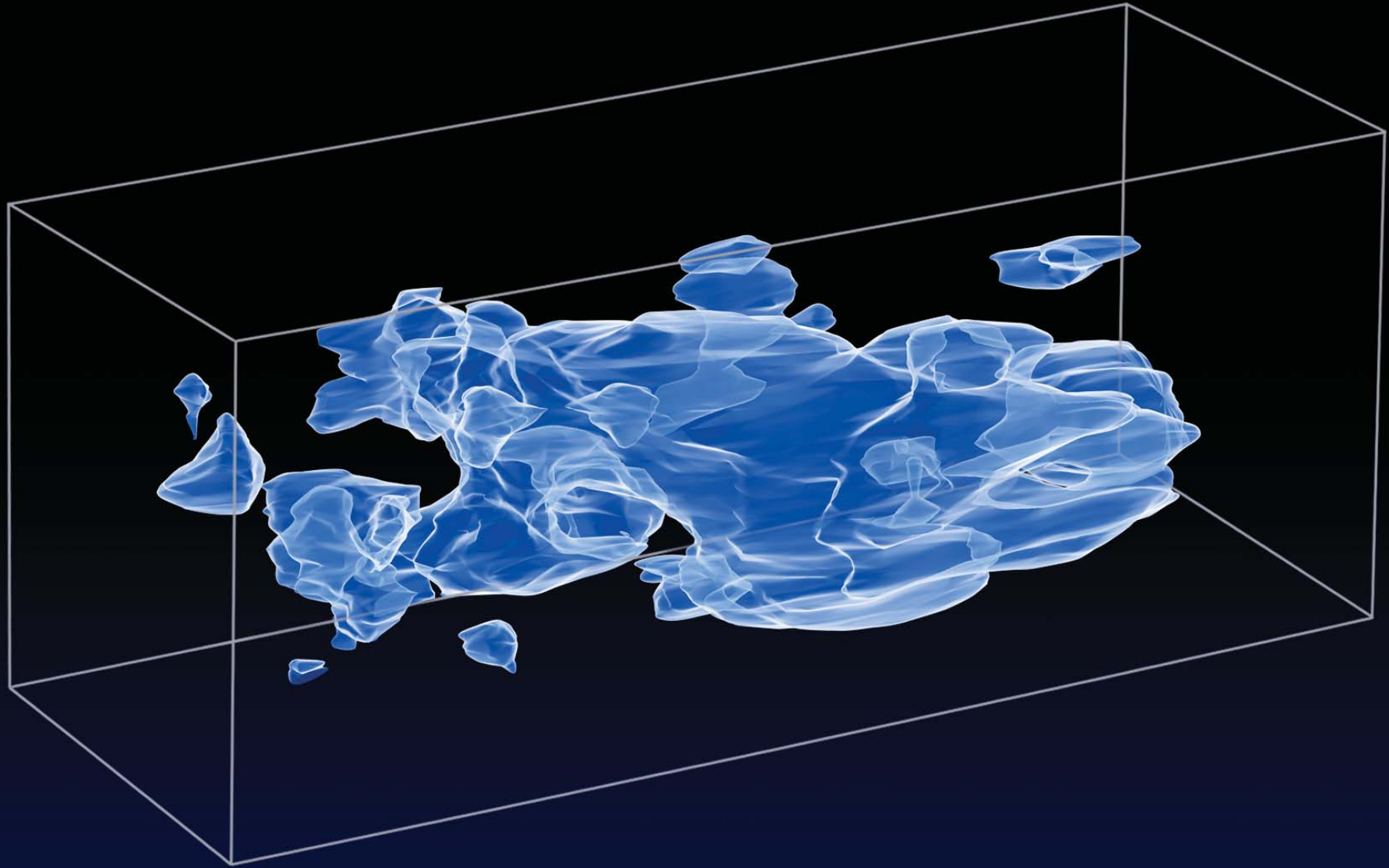
Dark matter

Light (galaxies)



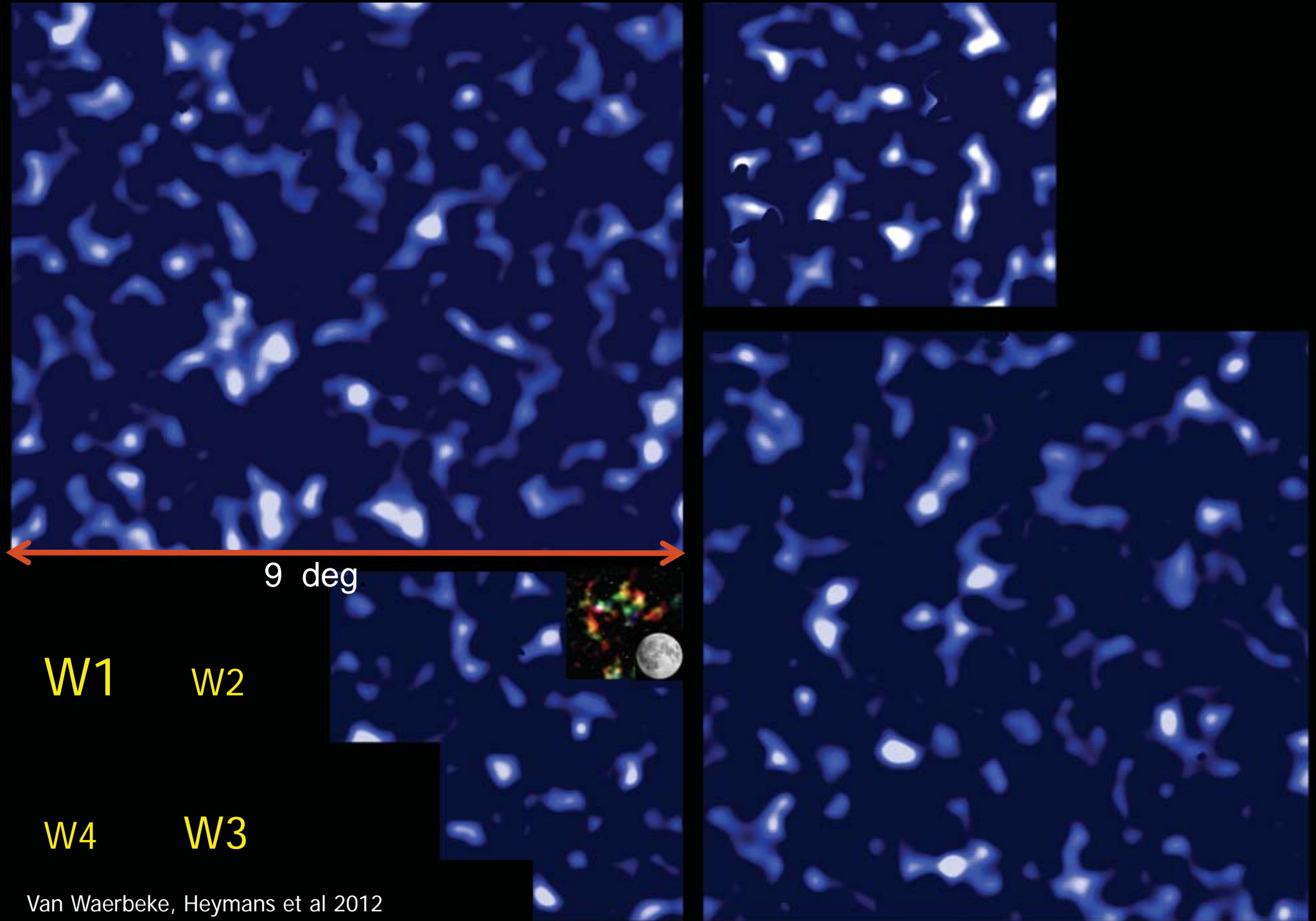
1.2 deg.

Cosmic shear and tomography with HST

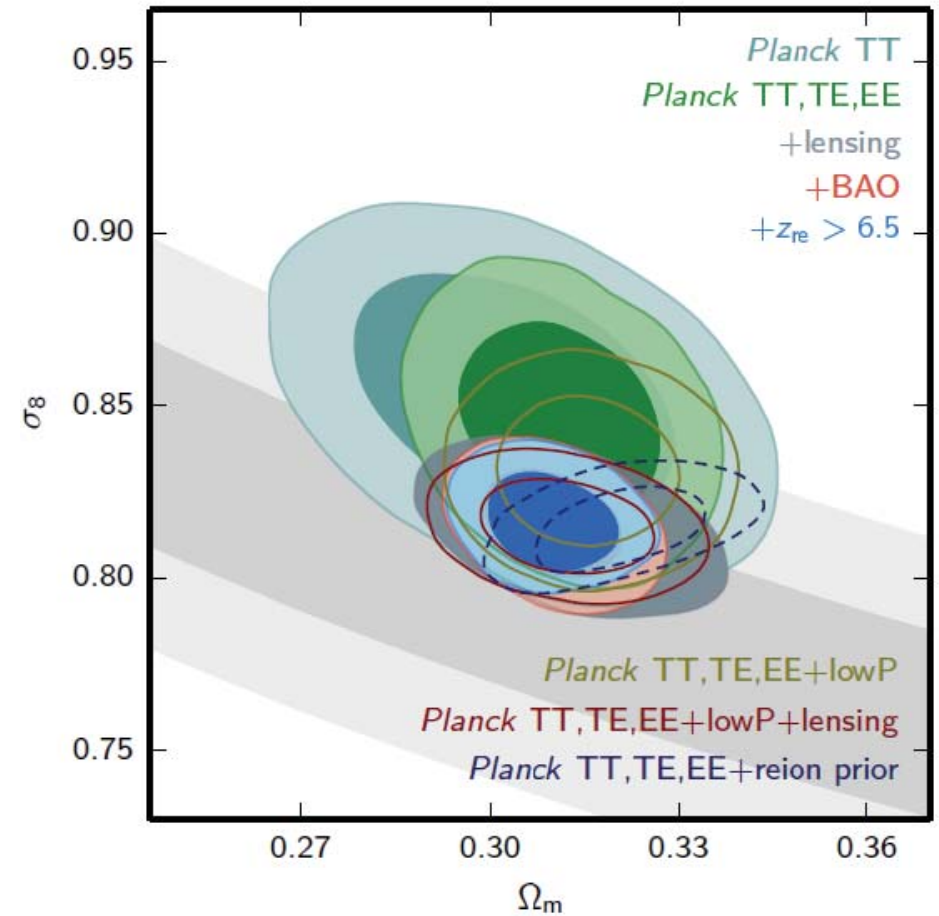
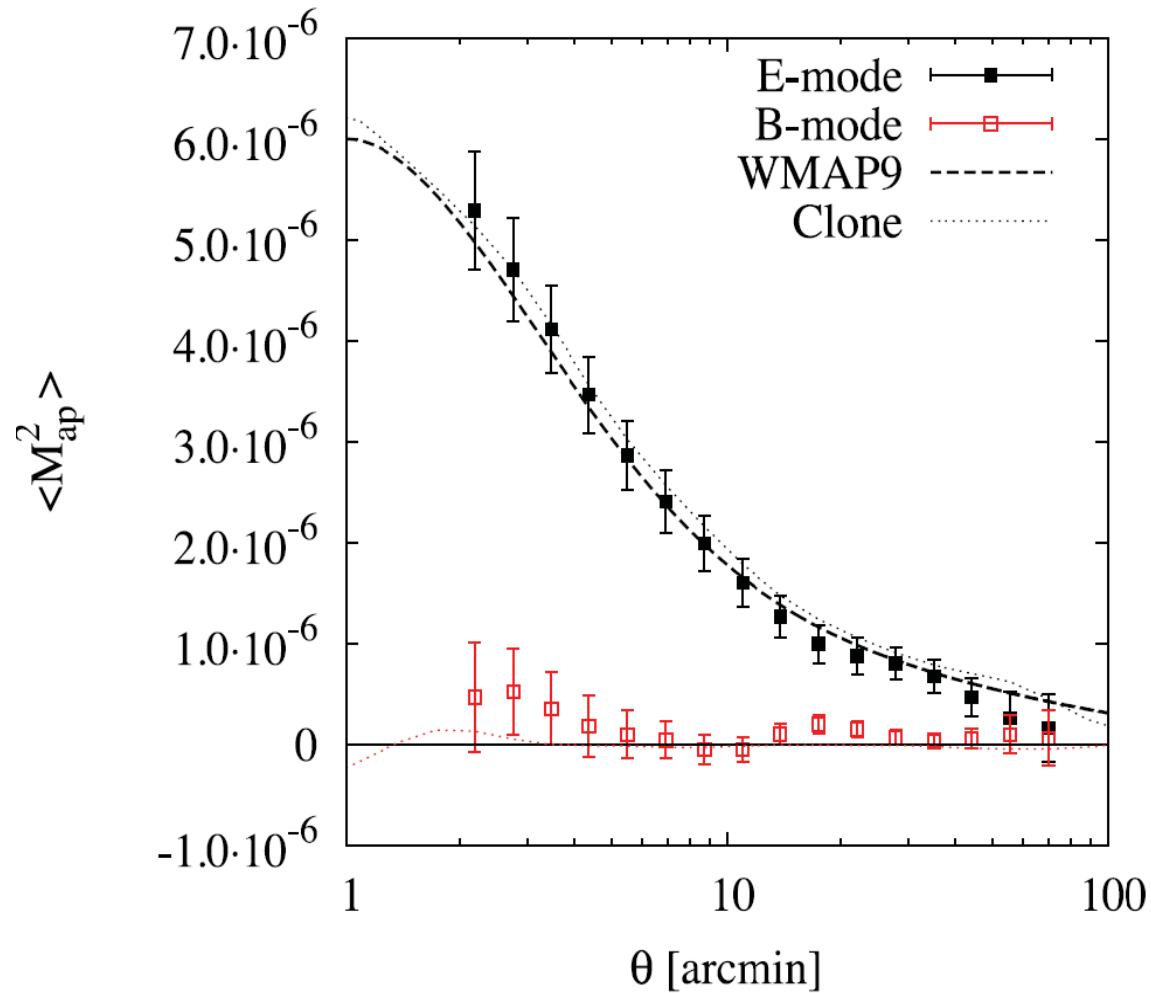


Massey et al 2007

CFHTLenS - mass maps Wide fields



CFHTLenS - Cosmic shear signal



Cosmology with WL ?

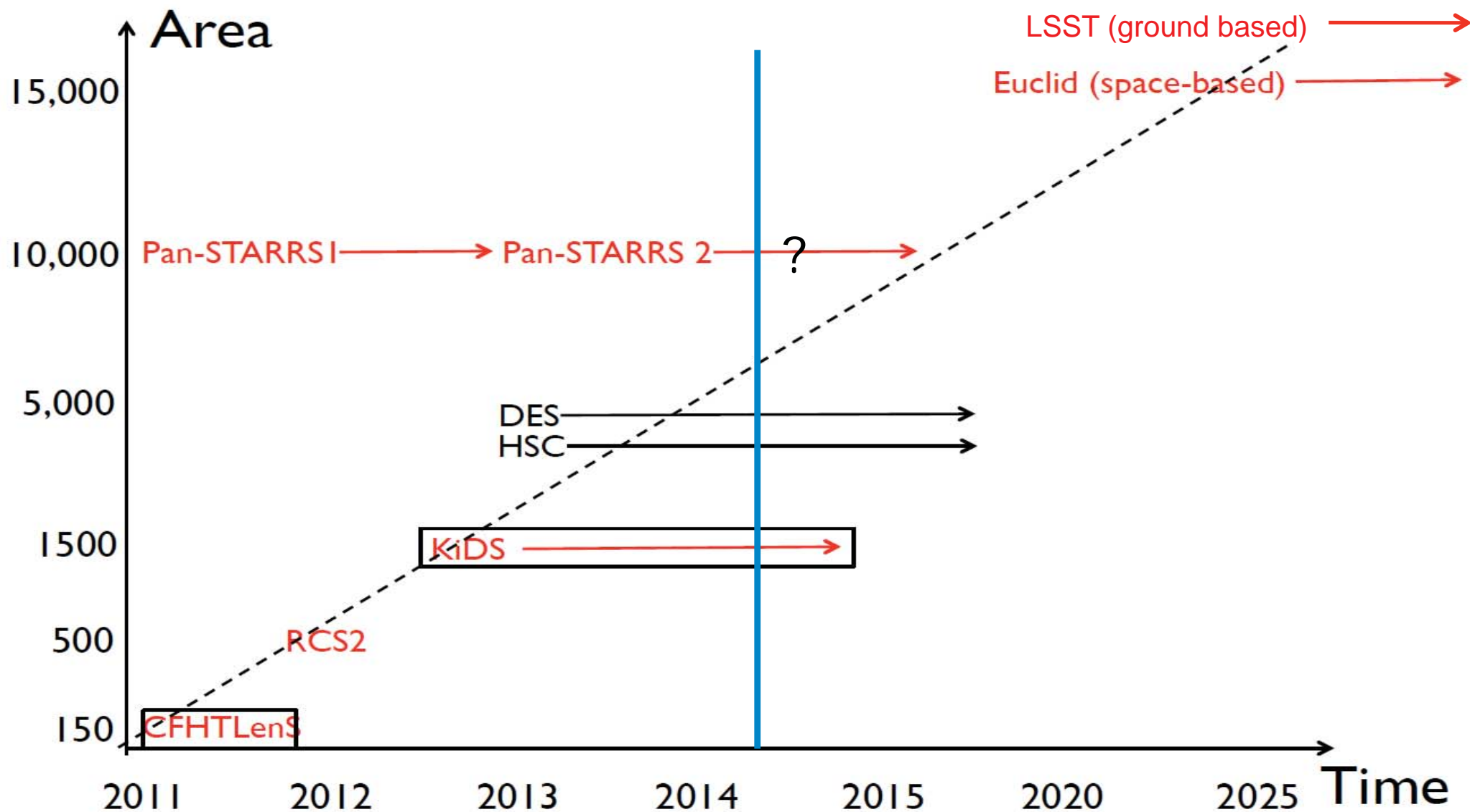
Weinberg et al 2013

| Reference | Telescope/instrument | Area (deg ²) | Number of galaxies | Result |
|-----------------------------|-------------------------------|--------------------------|--------------------|--|
| Bacon et al. (2000) | WHT/EEV-CCD | 0.5 | 27k | $\sigma_8 = 1.5 \pm 0.5$ (@ $\Omega_m = 0.3$) |
| Van Waerbeke et al. (2000) | CFHT/UH8K+CFH12K | 1.75 | 150k | Detection ^a |
| Wittman et al. (2000) | Blanco/BTC | 1.5 | 145k | Detection ^b |
| Rhodes et al. (2001) | HST/WFPC2 | 0.05 | 4k | $\sigma_8(\Omega_m/0.3)^{0.48} = 0.91^{+0.25}_{-0.30}$ |
| Van Waerbeke et al. (2001) | CFHT/CFH12K | 6.5 | 400k | $\sigma_8(\Omega_m/0.3)^{0.6} = 0.99^{+0.08}_{-0.10}$ (95%CL) ^f |
| Hoekstra et al. (2002) | CFHT/CFH12K +Blanco/Mosaic II | 53 | 1.78M | $\sigma_8(\Omega_m/0.3)^{0.55} = 0.87^{+0.17}_{-0.23}$ (95%CL) |
| Refregier et al. (2002) | HST/WFPC2 | 0.36 | 31k | $\sigma_8 = 0.94 \pm 0.14$ (@ $\Omega_m = 0.3$, $\Gamma = 0.21$) |
| Bacon et al. (2003) | Keck II/ESI +WHT | 1.6 | | $\sigma_8(\Omega_m/0.3)^{0.68} = 0.97 \pm 0.13$ |
| Brown et al. (2003) | MPG ESO 2.2m/WFI | 1.25 | | $\sigma_8(\Omega_m/0.3)^{0.49} = 0.72 \pm 0.09^{d,e}$ |
| Jarvis et al. (2003) | Blanco/BTC+Mosaic II | 75 | 2M | $\sigma_8(\Omega_m/0.3)^{0.57} = 0.71^{+0.12}_{-0.16}$ (2σ) |
| Hamana et al. (2003) | Subaru/SuprimeCam | 2.1 | 250k | $\sigma_8(\Omega_m/0.3)^{0.37} = 0.78^{+0.55}_{-0.25}$ (95%CL) |
| Rhodes et al. (2004) | HST/STIS | 0.25 | 26k | $\sigma_8(\Omega_m/0.3)^{0.46}(\Gamma/0.21)^{0.18} = 1.02 \pm 0.16$ |
| Heymans et al. (2005) | HST/ACS | 0.22 | 50k | $\sigma_8(\Omega_m/0.3)^{0.65} = 0.68 \pm 0.13$ |
| Massey et al. (2005) | WHT/PFIC | 4 | 200k | $\sigma_8(\Omega_m/0.3)^{0.5} = 1.02 \pm 0.15$ |
| Hoekstra et al. (2006) | CFHT/MegaCam | 22 | 1.6M | $\sigma_8 = 0.85 \pm 0.06$ @ $\Omega_m = 0.3$ |
| Semboloni et al. (2006a) | CFHT/MegaCam | 3 | 150k | $\sigma_8 = 0.89 \pm 0.06$ @ $\Omega_m = 0.3$ |
| Benjamin et al. (2007) | Various ^g | 100 | 4.5M | $\sigma_8(\Omega_m/0.3)^{0.59} = 0.74 \pm 0.04$ |
| Hetterscheidt et al. (2007) | MPG ESO 2.2m/WFI | 15 | 700k | $\sigma_8 = 0.80 \pm 0.10$ @ $\Omega_m = 0.3$ |
| Massey et al. (2007b) | HST/ACS | 1.64 | 200k | $\sigma_8(\Omega_m/0.3)^{0.44} = 0.866^{+0.085}_{-0.068}$ |
| Schrabback et al. (2007) | HST/ACS | 0.4 | 100k | $\sigma_8 = 0.52^{+0.11}_{-0.15}$ (stat) ± 0.07 (sys) @ $\Omega_m = 0.3^f$ |
| Fu et al. (2008) | CFHT/MegaCam | 57 | 1.7M | $\sigma_8(\Omega_m/0.3)^{0.64} = 0.70 \pm 0.04$ |
| Schrabback et al. (2010) | HST/ACS | 1.64 | 195k | $\sigma_8(\Omega_m/0.3)^{0.51} = 0.75 \pm 0.08$ |
| Huff et al. (2011) | SDSS | 168 | 1.3M | $\sigma_8 = 0.636^{+0.109}_{-0.154}$ @ $\Omega_m = 0.265^h$ |
| Lin et al. (2012) | SDSS | 275 | 4.5M | $\sigma_8(\Omega_m/0.3)^{0.7} = 0.64^{+0.08h}_{-0.12}$ |
| Jee et al. (2013) | Mayall+CTIO/Mosaic | 20 | 1M | $\sigma_8 = 0.833 \pm 0.034^i$ |
| Kilbinger et al. (2013) | CFHT/MegaCam | 154 | 4.2M | $\sigma_8(\Omega_m/0.27)^{0.6} = 0.79 \pm 0.03$ |

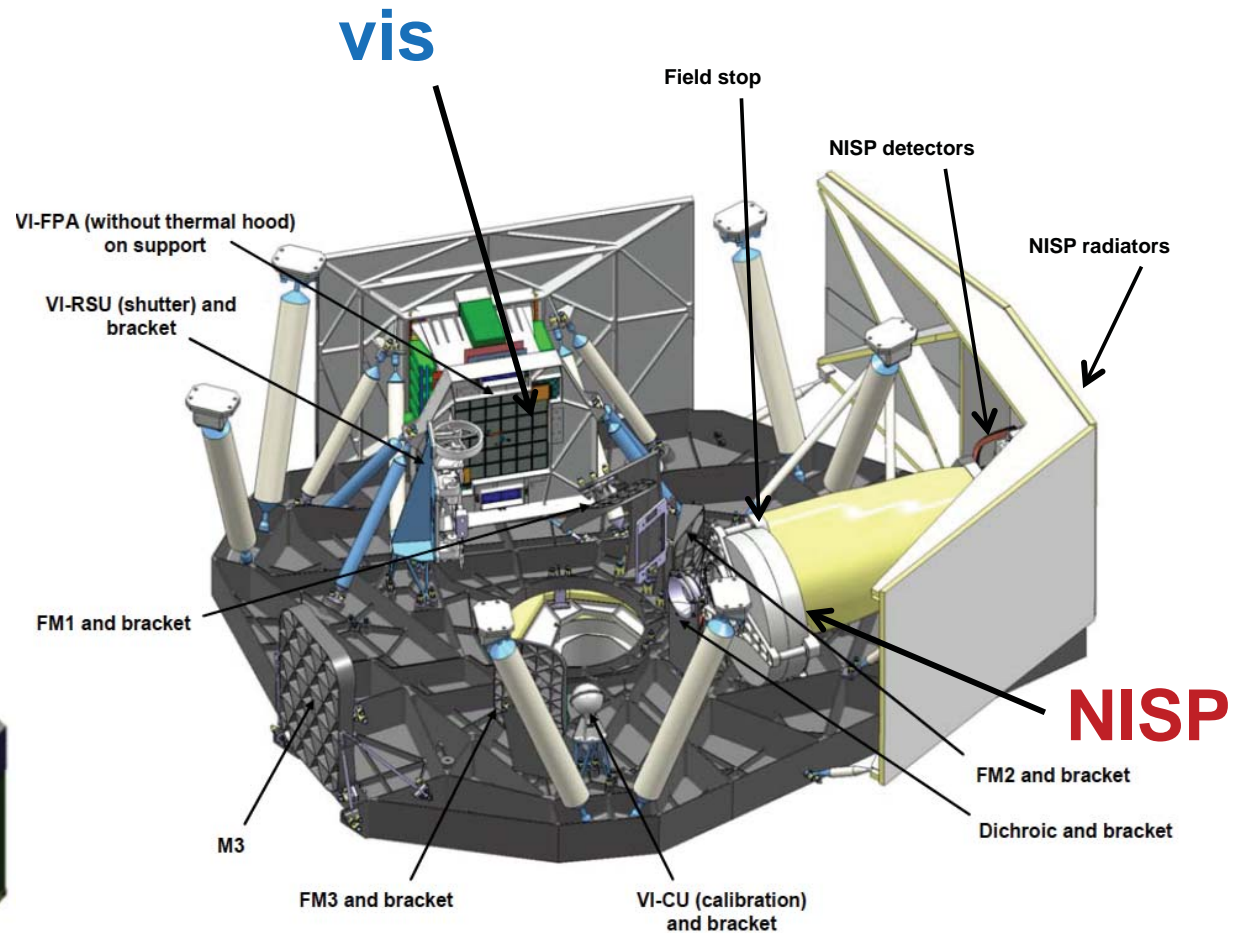
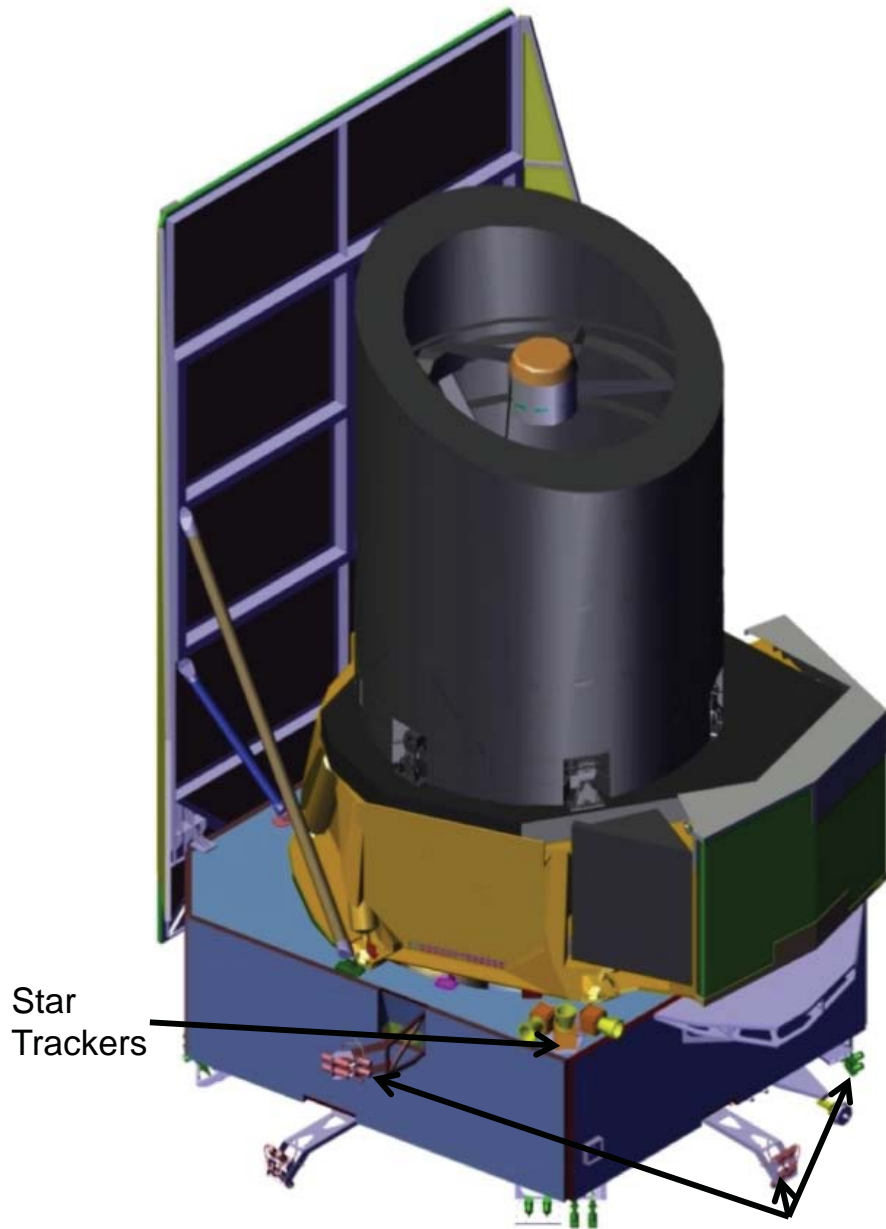
After first enthusiastic reactions: skepticism on reliability of WL data and cosmological interpretations: WL is a very hard (too hard?) technique

→ ... What Next ?

Future of cosmic shear surveys



Euclid



Common VIS and NIR FoV = 0.54 deg^2

Pointing error along the x,y axes = 25 mas over 700 s .

From Thales Alenia Space Italy, Airdus DS, ESA Project office and Euclid Consortium

Galaxy-lenses SLACS (~2010 - HST)



SLACS: The Sloan Lens ACS Survey

www.SLACS.org

A. Bolton (U. Hawai'i IfA), L. Koopmans (Kapteyn), T. Treu (UCSB), R. Gavazzi (IAP Paris), L. Moustakas (JPL/Caltech), S. Burles (MIT)

Image credit: A. Bolton, for the SLACS team and NASA/ESA

SLACS

Euclid after 2 months
(66 months expected)



Summary

Gravitational lensing

- Can probe the distribution of dark matter from galaxies to large scale structures of the Universe almost directly.
- Is an independent method, beside X-ray or dynamical ones
- Show evidence of dark matter in
 - [MACHOS in our galaxy \(microlensing: no time to discuss here\)](#)
 - Other galaxies (Strong lensing, Weak lensing)
 - Groups and Clusters of galaxies (SL, WL)
 - Superclusters of galaxies (WL)
 - Large Scale Structure (WL)

Summary

- Gravitational lensing confirms that a Universe without dark matter can hardly explain observations
- Modified gravity is still an option but not favoured
- Weak and/or Strong lensing data agree with NFW and SIS, but favours NFW-like radial profiles
- All data compatible with Lambda-CDM predictions
- Cosmic shear is detected, favours lambda-CDM, but detection and measurements very hard and systematics still an issue
- Likely : WL still have to improve
 - Much more statistics: number of galaxies, wave number
 - Improve shear measurement → space
 - Numerical simulations for baryon physics (small scales)